

SIMULATION OF GLYCEROL STEAM REFORMING

A DISSERTATION

*Submitted in partial fulfilment of the
requirements for the award of the degree*

of

INTEGRATED DUAL DEGREE

(Bachelor of Technology & Master of Technology)

in

CHEMICAL ENGINEERING

(With specialization in Hydrocarbon Engineering)

By

SANMAT JAIN



**DEPARTMENT OF CHEMICAL ENGINEERING
INDIAN INSTITUTE OF TECHNOLOGY, ROORKEE
ROORKEE-247667
JUNE-2013**

Candidate's Declaration

I hereby declare that the work, which is being presented in the dissertation entitled “**Simulation of Glycerol Steam Reforming**” submitted in the partial fulfilment of the requirements for the award of the Integrated Dual Degree (Bachelor of Technology & Master of Technology) in Chemical Engineering with specialization in “Hydrocarbon Engineering”, submitted in the Department of Chemical Engineering, Indian Institute of Technology Roorkee, Roorkee, is an authentic record of my own work carried out during the period from May 2012 to June 2013 under supervision of **Dr. V. K. Agarwal**, Professor, Department of Chemical Engineering, Indian Institute of Technology Roorkee, Roorkee, India.

The matter presented in this report has not been submitted by me for the award of any other degree of this or any other institute.

Date:

Sanmat Jain

Place: Roorkee

Enrolment No.08210015

Certificate

This is to certify that the above statement made by the candidate is correct to the best of my knowledge and belief.

Dr. V. K. Agarwal
Professor and Head of Department
Department of Chemical Engineering
Indian Institute of Technology Roorkee
Roorkee, Uttarakhand- 247667
India

Acknowledgement

I express my deep sense of gratitude to my guide **Dr. V. K. Agarwal**, Professor and Head, Department of Chemical Engineering, Indian Institute of Technology Roorkee, Roorkee, for his keen interest, constant guidance and encouragement throughout the course of this work, his experience, assiduity and deep insight of the subject held this work always on a smooth and steady course.

Above all, I want to express my heartiest gratitude to The Almighty, my parents (Mrs. Sushila Devi Jain and Mr. Lakhmi Chand Jain), for their love, faith and support for me, which has always been a constant source of inspiration.

Date:

Sanmat Jain

Place: Roorkee

ABSTRACT

A two dimensional (2D) transient simulation is carried out to simulate a glycerol steam reforming reaction in a fluidized bed reactor for hydrogen production using commercially available simulation software Fluent 13.0 (Ansys). The Eulerian-Eulerian two fluid approach with an additional equation for species transport is used to model the reactor. Three step reaction mechanism is used to represent reactions occurring in the reactor and which are incorporated in model by using laminar finite rate model available in fluent. Gidaspow drag model is used to determine the interactions occurring between gas and solid phase in the reactor.

The results show that the model can satisfactorily represent the glycerol steam reforming reactor. Hydrodynamics of reactor showed that clusters of solid phase are formed thus making fluidized heterogeneous in nature. Thus in order to ensure proper mixing continuous agitation has to be done. Product gases mainly included hydrogen (H_2), carbon di-oxide (CO_2), methane (CH_4) and in very less amount carbon mono-oxide (CO). Glycerol conversion and hydrogen formation increases with increasing steam to carbon ratio (s/c) and increase in temperature. Also, with increasing inlet feed mixture velocity glycerol conversion and hydrogen formation decreases.

Contents

Candidate's Declaration	i
Acknowledgement	ii
ABSTRACT	iii
Table of figures	vi
List of tables	vii
NOMENCLATURE.....	viii
CHAPTER 1	1
1. Introduction	1
1.1 Glycerol and its source.....	1
1.2 Glycerol to hydrogen conversion processes	2
1.3 Fluidised bed reactor	3
1.4 Motivation.....	4
1.5 Objective	4
CHAPTER 2	5
2 Literature Review.....	5
2.1 Thermodynamic analysis.....	5
2.2 Kinetics study on catalyst.....	7
2.3 Modeling and simulation	11
CHAPTER 3	14
3 CFD Modeling of fluidized bed reactor	14
3.1 Approaches to Gas-Solid Fluidization Modeling	14
3.2 Computational flow model	15
3.2.1 Gas-solid flow equations.....	15
3.2.2 Reaction model	20
CHAPTER 4	21
4 Solution Methodology	21
4.1 Problem statement	21
4.2 Numerical Methodology	23
CHAPTER 5	26
5 Results and Discussions	26

5.1	Hydrodynamics of fluidized bed	26
5.1.1	Pressure drop across the bed	26
5.1.2	Contours of volume fraction of solid phase in reactor	28
5.2	Reactant conversion and product yield	30
5.2.1	Glycerol and steam conversion.....	30
5.2.2	Product formation.....	31
5.3	Effect of process variables	34
5.3.1	Variation of inlet mixture velocity	34
5.3.2	Variation of steam to carbon ratio (s/c) in the inlet mixture.....	40
5.3.3	Variation of reaction temperature.....	45
CHAPTER 6		50
6	Conclusion and Recommendations.....	50
6.1	Conclusion.....	50
6.2	Recommendations	51
CHAPTER 7		52
7	References	52

Table of figures

Figure 4.1: Reactor set up	21
Figure 4.2: Grid and patch field.	23
Figure 5.1: Pressure drop variation with flow time.	27
Figure 5.2: Contours of solid volume fraction with flow time.	29
Figure 5.3: Fractional conversion of glycerol and steam with flow time.....	31
Figure 5.4: Concentration of product gases in outlet.	32
Figure 5.5: Concentration of CO in outlet.....	32
Figure 5.6: Product gas concentration with flow time ($v=0.5\text{m/s}$, $s/c=2:1$, $T=600^{\circ}\text{C}$).....	34
Figure 5.7: Glycerol concentration at outlet with flow time ($v=0.5\text{m/s}$, $s/c=2:1$, $T=600^{\circ}\text{C}$).....	35
Figure 5.8: Glycerol conversion with flow time ($v=0.5\text{m/s}$, $s/c=2:1$, $T=600^{\circ}\text{C}$).....	35
Figure 5.9: Product gases concentration with flow time ($v=0.55\text{m/s}$, $s/c=2:1$, $T=600^{\circ}\text{C}$).	36
Figure 5.10: Glycerol concentration at outlet with flow time ($v=0.55\text{m/s}$, $s/c=2:1$, $T=600^{\circ}\text{C}$).....	36
Figure 5.11: Glycerol conversion with flow time ($v=0.55\text{m/s}$, $s/c=2:1$, $T=600^{\circ}\text{C}$).....	37
Figure 5.12: Product gases concentration with flow time ($v=0.6\text{m/s}$, $s/c=2:1$, $T=600^{\circ}\text{C}$).	37
Figure 5.13: Glycerol concentration in outlet with flow time ($v=0.6\text{m/s}$, $s/c=2:1$, $T=600^{\circ}\text{C}$).....	38
Figure 5.14: Glycerol conversion with flow time ($v=0.6\text{m/s}$, $s/c=2:1$, $T=600^{\circ}\text{C}$).....	38
Figure 5.15: Hydrogen concentration in outlet variation with inlet mixture velocity.	39
Figure 5.16: Glycerol conversion variation with inlet velocity.	40
Figure 5.17: Product gases concentration with flow time ($v=0.5\text{m/s}$, $s/c=3:1$, $T=600^{\circ}\text{C}$).	41
Figure 5.18: Glycerol concentration in outlet with flow time ($v=0.5\text{m/s}$, $s/c=3:1$, $T=600^{\circ}\text{C}$).	41
Figure 5.19: Glycerol conversion with flow time ($v=0.5\text{m/s}$, $s/c=3:1$, $T=600^{\circ}\text{C}$).....	42
Figure 5.20: Product gases concentration with flow time ($v=0.5\text{m/s}$, $s/c=4:1$, $T=600^{\circ}\text{C}$).	42
Figure 5.21: Glycerol concentration in outlet with flow time ($v=0.5\text{m/s}$, $s/c=4:1$, $T=600^{\circ}\text{C}$).	43
Figure 5.22: Glycerol conversion in outlet with flow time ($v=0.5\text{m/s}$, $s/c=4:1$, $T=600^{\circ}\text{C}$).....	43
Figure 5.23: Variation of hydrogen concentration in outlet with s/c ratio.....	44
Figure 5.24: Variation of Glycerol conversion with s/c ratio	45
Figure 5.25: Product gases concentration with flow time ($v=0.5\text{m/s}$, $s/c=2:1$, $T=650^{\circ}\text{C}$)	46
Figure 5.26: Glycerol conversion with flow time ($v=0.5\text{m/s}$, $s/c=2:1$, $T=650^{\circ}\text{C}$).....	46

Figure 5.27: Product gases concentration with flow time ($v=0.5\text{m/s}$, $s/c=2:1$, $T=700^{\circ}\text{C}$)	47
Figure 5.28: Glycerol conversion with flow time ($v=0.5\text{m/s}$, $s/c=2:1$, $T=700^{\circ}\text{C}$).....	47
Figure 5.29: Variation of hydrogen concentration in outlet with temperature.	48
Figure 5.30: Variation of glycerol conversion with temperature	49

List of tables

Table 4.1: Glycerol steam reforming reactor set up	22
Table 4.2: 2D grid of the reactor	24
Table 4.3: Operating and boundary conditions	24
Table 4.4: Simulation set up.....	25
Table 4.5: Values of kinetic parameters for reactions.	25
Table 5.1: Comparison of experimental and simulated results	33

NOMENCLATURE

ρ_k	Density of phase k= g (gas), s (solid)
ϵ_k	Volume fraction of phase k= g (gas), s (solid)
v_k	Velocity of phase k= g (gas), s (solid)
$\mu_{g,l}$	Gas phase laminar viscosity
P	Pressure (Pa)
d_p	Particle diameter, (m)
t	Time, (s)
u	Velocity component in radial direction, (m/s)
v	Velocity component in axial direction, (m/s)
θ_s	Solid phase granular temperature (m^2/s^2)
τ_i	Viscous stress tensors, (Pa),
K_s	Diffusion coefficient of granular temperature
Re	Particle Reynolds number
L	Height along axial (m)
C_D	Drag coefficient
e_{ss}	Coefficient of restitution between particles of solid phase s
g	Vector representation of acceleration due to gravity, 9.81 m/s^2
g_o	Radial distribution function between particles belonging to a solid phase s
K_{sg}	Momentum exchange coefficient between phase s and phase g
γ_s	Collision dissipation of granular temperature

Greek Letters

β	Interphase exchange coefficient ($\text{kg/m}^3 \text{ s}$)
ϵ	Volume fraction (-)
γ	Dissipation of fluctuating energy (kg/m/s^3)
Θ	Granular temperature (m^2 / s^2)
μ	Shear viscosity (Pa.s)
ξ	Bulk viscosity (Pa.s)
ρ	Density (kg/m^3)
τ	Shear stress tensor (N/m^2)
Φ	Angle of internal friction ($^\circ$)

1. Introduction

1.1 Glycerol and its source

Glycerol is oxygenated hydrocarbon with chemical formula $C_3H_8O_3$. It has three hydroxyl groups, one on each carbon atom with C/H ratio equal to one. It is non-toxic and biodegradable. . It is also not suitable for burning in diesel and petrol engines.

Glycerol can be produced by hydrogenolysis from propylene oxide and from glucose by fermentation. It can also be obtained as side product of some of the industrial processes such as

- soap manufacturing via saponification of fats process,
- biodiesel production via trans-esterification reaction process and
- lignocellulose to ethanol production process

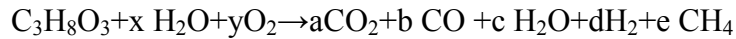
In biodiesel production process about 10% of vegetable oil or animal fat are converted to glycerol. In the world presently there is large amount of glycerol produced each year as a by-product of above mentioned industrial processes. So, it has become quite cheap and in future might also become a waste a waste problem. Presently, glycerol is being used in different industries namely chemical, food, pharmaceutical and others. In future, glycerol can also become a potential source of hydrogen.

As we know that the conventional sources of energy are limited and they also emit greenhouse gases on combustion. Now, we have started to feel the effect of climate change like extreme weather condition, change in distribution and intensity of rainfall. Worldwide efforts are being made to curb the climate change phenomena with greater restrictions on use of fossil fuels and towards renewable sources of energy. Hydrogen is one such alternative fuel which is thought as a future fuel. Producing hydrogen from glycerol would be a renewable environmentally friendly source of energy. Advantages of using hydrogen as a fuel:

- 1) It has high energy content as compared to other fuels.
- 2) It does not produce greenhouse gases like CO_2 and CO on combustion.
- 3) Hydrogen production from renewable source is also CO_2 neutral.

1.2 Glycerol to hydrogen conversion processes

Hydrogen from glycerol can be obtained from various glycerol reforming processes. Glycerol reforming is an endothermic reaction and can be given as follows :



Glycerol reforming is of different types depending upon the heat source and oxidizing agent used. They are partial oxidation, autothermal reforming and steam reforming.

Steam reforming process

The steam reforming process uses steam as a oxidizing agent at high temperature (800 °C) and low pressure (0.1 MPa). Glycerol steam reforming can be represented by following equation:



The primary reactions comprises of are glycerol decomposition and water gas shift reactions:



Because of the methanation of CO and CO₂, the H₂ yield is reduced:



Major disadvantages are high energy requirement, catalyst deactivation and by-product formation.

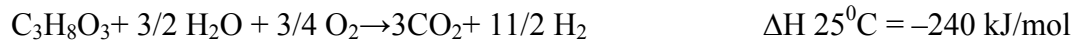
Partial oxidation process

The catalytic partial oxidation process is an exothermic process. It uses an oxygen as an oxidizing agent and source of required heat. The reaction can be represented as:



Autothermal reforming

In Auto-thermal reforming both steam and oxygen is used and there is no requirement of any external heat. Auto-thermal reforming of glycerol is represented by:



It can be seen that H_2 produced in steam reforming reaction is maximum than other reactions. Steam reforming of glycerol can produce up to 7 mole of hydrogen theoretically from one mole of glycerol. This makes it a potentially economical and environmentally friendly option.

1.3 Fluidised bed reactor

In fluidization solids behave like a fluid due to contact of gas or liquid. Fluidized bed reactor is used for large scale industrial chemical and biochemical processes.

Advantages

- It has excellent gas-solid contacting and particle mixing.
- Nearly isothermal conditions can be maintained throughout the reactor.
- It provides high gas-solid and solid-wall heat transfer.

Disadvantages

- by-passing,
- channeling and
- attrition of solid particles thus leading to loss of fines from the reactor.

Bubbling fluidized bed reactor and circulating fluidized reactor are the most common used reactor in the industry.

The steam reforming of glycerol in a fluidized bed reactor involves complex flows and reactions occurring in the reactor. Simulating the glycerol steam reforming reaction in a fluidized bed reactor can depend on the ability to predict exactly the hydrodynamics and multiple reactions occurring in the reactor. Computational fluid dynamics (CFD) technique can be an effective tool to predict the exact behavior of the glycerol steam reforming reaction occurring in a fluidized bed.

1.4 Motivation

Biodiesel production has increased in the recent past and with that large amount of crude glycerol is also produced as a byproduct. Crude glycerol has several impurities namely inorganic salts, methanol, free fatty acids and other organic material. This crude glycerol is poor fuel and also not suitable for blending with petrol and diesel. Therefore, this crude glycerol is refined by distillation and then sold to food, pharmaceutical, and cosmetic industries. Increased glycerol production and limited option for its disposal has resulted into an unexpected fall in glycerol prices, thus new ways have to be found out for its conversion to useful products

As hydrogen is a clean fuel, conversion of glycerol to hydrogen can be the attractive way to make use of glycerol, as 7 moles of hydrogen can be produced per mole of glycerol by steam reforming of glycerol. This makes it a potentially economical and friendly to environmental option.

In view of the above, I have decided to work on Simulation of glycerol steam reforming.

1.5 Objective

- To formulate the model for glycerol steam reforming reaction in a fluidized bed reactor.
- To examine the model with experimental data available in literature.
- To determine the effect of variation in process variables namely steam to carbon ratio, inlet velocity of mixture and temperature on hydrogen production and glycerol conversion.

2 Literature Review

Biodiesel has become popular as a fuel and for fuel blending due to its renewable nature and its environmental benefits. The different processes of biodiesel production are direct use and blending, thermal cracking (pyrolysis), micro-emulsions and transesterification reaction. Transesterification of vegetable oils and animal fats is the most common method of biodiesel production. Glycerol is the by-product of transesterification reaction of biodiesel production. Glycerol, obtained from renewable sources, conversion to hydrogen through steam reforming is seen as a very good option. Thus literature review of thermodynamic analysis, reaction kinetics on different catalyst and modeling and simulation of glycerol steam reforming in reactor is done and given below.

2.1 Thermodynamic analysis

The steam reforming of glycerol involves complex set of reactions leading to the formation of various reaction intermediate byproducts. These intermediate byproducts come in product stream thus decreasing the hydrogen purity. Furthermore, hydrogen yield depends on several process variables, such as temperature, pressure and ratio of reactants in the feed. The first step is to understand the effects of variables which can be done through complete thermodynamic analysis.

Hao Wang et al.[2] In this study, glycerol autothermal reforming for production of hydrogen(used in fuel cell application) is investigated through thermodynamics analysis. Minimization of gibbs free energy technique is used to do the equilibrium calculations for a range of process variables namely temperature 700 K – 1000 K, $O_2/C_3H_8O_3$ ratio 0.0–3.0 and $H_2O/C_3H_8O_3$ ratio from 1–12. Most favorable conditions for hydrogen production are temperature of 900-1000 K, steam to glycerol ration of 9-12 and oxygen to glycerol ratio of 0.0-0.4. Maximum number of moles of hydrogen produced is 5.62 at 900 K and 5.43 at 1000 K at these thermoneutral conditions. Also, at these condition methane and carbon formation can be eliminated.

Sushil Adhikari et al.[3] In this paper, thermodynamic analysis of steam reforming of glycerol is done. A thermodynamic equilibrium analysis has been performed over the ranges of process variable ranges: pressure (1–5) atmosphere, temperature (600–1000K), and steam-to-glycerol feed ratio 1:1–9:1. The minimization of Gibbs free energy technique is used for equilibrium calculations. The study showed that the best conditions for hydrogen production are at a temperature greater than 900K, atmospheric pressure, and a molar ratio of steam to glycerol of 9:1. At these conditions carbon formation and methane production is minimized.

Haisheng Chen et al.[17] In this work, the thermodynamic study of steam reforming of glycerol for hydrogen production with adsorption is performed using the minimization of the Gibbs free energy principle. Various process variables are there which affects the reforming reactions and carbon formation thus the effects of pressure (1-4 bar), temperature (600-1000K), water to glycerol feed ratio (3:1-12:1) and molar ratio of carrier gas to feed reactants (1:1-1:5) has been investigated. The results show that most favorable temperature range for hydrogen formation is 800-850 K in presence of adsorbent which is about 100 K lower than not using the adsorbents. Glycerol conversion can be increased by using CO₂ adsorbents and the moles of hydrogen produced from one mole of glycerol can be increased from 6 to 7 using CO₂ adsorbents. Other favorable conditions for hydrogen production are low pressure although high pressure would be suitable for CO₂ adsorption, water to glycerol ratio of 9:1. Using high values of water to glycerol ratio gives marginal benefits and lower values of water to glycerol ratio leads to carbon formation.

Yunhua Li et al.[19] In this work thermodynamic analysis of glycerol steam reforming with CO₂ adsorption has been studied using the minimization of Gibbs free energy technique. Using CaO for CO₂ adsorption has potential advantage as water gas shift reactor is not required for high purity hydrogen (which is required for fuel cell applications). Results show that optimum conditions are atmospheric pressure, temperature of 900 K, the water-to-glycerol molar ratio of 4, the CaO-to-glycerol molar ratio of 10. Complete glycerol conversion with no coke formation can be achieved at these optimum conditions. Concentrations of hydrogen and carbon mono oxide are found to be 96.80% and 0.73% respectively. It is also reported that the energy

efficiency is higher for CO₂ adsorption enhanced steam reforming reactions than without adsorption under identical conditions.

2.2 Kinetics study on catalyst

Glycerol steam reforming reactions can be carried out on different catalyst which changes the product gas distribution and the conversion of glycerol obtained. Some researchers have done experiments using different catalyst. So, in this section a review of different glycerol steam reforming reaction catalyst is done.

Baocai Zhang et al.[4] In this work, glycerol steam reforming reaction has been studied over ceria supported catalysts (Ir, Co and Ni). Results show that ceria supported Ir catalyst to be more active and selective towards hydrogen production from the steam reforming reactions of glycerol. Glycerol steam reforming reaction in presence of Ir/CeO₂ catalyst showed good performance with hydrogen selectivity and glycerol conversion of more than 85% and 100% respectively at 400⁰C

Francisco Pompeo et al.[5] In this study, glycerol steam reforming reaction for hydrogen production has been investigated on Pt catalysts (with different supports) at temperature less than 450⁰C. Results showed that there was a strong effect of support on the behavior of catalyst. Catalyst with acidic material supports showed low activity towards gas production. Some side products are produced due to condensation and dehydration reaction. There was formation of coke due to these side reactions thus leading deactivation of catalyst. On the other side, the catalyst with neutral material support showed excellent activity to gas production with high selectivity to hydrogen and also very stable catalyst with time.

V. Chiodo et al.[6] In this study, steam reforming of glycerol has been investigated on Rh and Ni supported catalyst for hydrogen or syngas production. According to results obtained at temperature above 720 K glycerol decomposes due to pyrolysis before reaching the catalyst surface. Among the two catalyst Rh/Al₂O₃ catalyst was found to be more active and stable than Ni supported catalysts. Apart from catalyst used and operating temperature, reaction is greatly affected by formation of coke. This coke formation is mainly promoted by olefins which are produced by glycerol decomposition at high temperature. Thermodynamics also shows that

reaction should be operated at high temperature for more hydrogen production but this temperature should not be more than 923 K which would lead to the formation of encapsulated carbon thus affecting the catalyst activity.

Binlin Dou et al.[7] In this study pyrolysis of crude glycerol obtained from biodiesel plant is investigated using thermogravimetry analysis. The thermogravimetric kinetics of pyrolysis reaction has been derived. Water and methanol presence in crude glycerol catalyze its decomposition. Crude glycerol decomposes at a temperature less than 500 K which is lower than that for pure glycerol. Decomposition of crude glycerol also leaves large mass fraction of pyrolysis residue which is about 15%. The first law power model correctly predicted the pyrolysis of crude glycerol. The activation energies obtained for decomposition of crude and pure glycerol shows the difference of 10-30 kJ/mol. This difference in activation energy can be attributed to catalytic effect of water and methanol present in crude glycerol.

Kaihu Hou et al.[8] This is the experimental study of methane steam reforming reaction followed by water gas shift reaction on a Ni/ α -Al₂O₃ catalyst in an integral reactor. The results showed that both carbon mono-oxide (CO) and carbon di-oxide (CO₂) are primary products. At low product concentration the methane conversion rate is proportional to partial pressure of methane. Surface reactions occurring between the adsorbed species are found to be the rate controlling step which is determined by the effect of total pressure on initial reaction rates. A model for kinetics of methane steam reforming has been determined using the method of parameter estimation and model discrimination.

Methane steam reforming is found to be first order with respect to methane at low conversion and low temperature as methane conversion being proportional to contact time and partial pressure of methane. Product distribution from methane steam reforming reaction is largely effected by temperature and steam to methane ratio while pressure seems to have no noticeable effect on it. The result shows that low temperature and high steam to methane ratio are favorable for hydrogen and synthesis gas production. At low temperature carbon di-oxide rate of formation is more than carbon mono-oxide rate of formation, and tending to get reduced with temperature.

Sushil Adhikari et al.[12] This work is regarding the characterization and testing of catalyst for glycerol steam reforming reaction for hydrogen generation. In this work fourteen catalysts are prepared on ceramic foam monoliths using incipient wetness technique. The catalytic effect of these fourteen catalysts on hydrogen selectivity and glycerol conversion is being determined under the temperature range of 600 to 900⁰C. The effect of process variables steam to glycerol ratio, feed inlet flow rate and metal bonding is determined on best catalysts. The Ni/Al₂O₃ and Rh/CeO₂/Al₂O₃ are found to be the best catalyst under the operating conditions investigated. Higher water to glycerol ratio was beneficial for higher H₂ selectivity and C₃H₈O₃ conversion. At temperature 900⁰C, 0.15 ml/min feed rate and water to glycerol ratio of 9:1 the selectivity of hydrogen obtained for Ni/Al₂O₃ and Rh/CeO₂/Al₂O₃ are about 80% and 71% respectively. Glycerol conversion increased with increase metal bonding but selectivity of hydrogen remained unaffected. Glycerol conversion of 94% is reported in both the catalysts at 3.5 wt% of metal loading.

Sushil Adhikari et al.[13] This paper gives the kinetic parameters for steam reforming of glycerol on Ni/CeO₂ catalyst. A mathematical model is developed which predicted the conversion of glycerol within 6.7% deviation limits from experimental value. The values of 0.233 reaction order with respect to glycerol and 103.4 kJ/mol activation energy for glycerol steam reforming reaction over Ni/CeO₂ catalyst are reported.

Parag N. Sutar et al.[14] This study considered the Pt/C catalyst for kinetics of glycerol steam reforming reaction. Fixed bed reactor is used for obtaining the glycerol conversion rate with time which is required for determining the kinetic parameters using integral method analysis. The first order reaction kinetics with respect to glycerol has been reported under the operating conditions of temperature from 623 to 673 K and space time from 0.39 to 1.56 g h/mol. The value kinetic parameter k at 673 K was given to be 1.1x10⁵cm³/gcat h. The model predicted the glycerol conversion in close agreement with the experimental values. Hydrogen yield increased with increasing the temperature, water to glycerol molar ratio and residence time inside the reactor.

Ravi Sundari et al.[15] In this work Ru/Al₂O₃ catalyst has been investigated for its effect on glycerol steam reforming reaction in a fixed bed reactor. The range of temperature in the experiment was 350 to 500 °C. The results show that the reaction order with respect to glycerol is one. The reaction rate constant and activation enthalpy at 500 °C are 4.2×10⁵ cm³/(gcat h) and 21.2 kJ/mol.

Sushil Adhikari et al.[18] Three catalysts (Ni/CeO₂, Ni/MgO, and Ni/TiO₂) of Ni with different supports have been investigated in this study for hydrogen production glycerol steam reforming reaction. Among the three, Ni/CeO₂ has the highest surface area of 67.0m²/g. Ni/CeO₂ is found to be the best performing catalyst than the other two under the investigated experimental conditions. At temperature 600°C, water to glycerol molar ratio 12:1 and feed flow rate of 0.5 mL/min hydrogen selectivity for Ni/CeO₂, Ni/MgO and Ni/TiO₂ are 74.7%, 38.6% and 28.3% respectively.

Binlin Dou et al.[9] In this paper, glycerol steam reforming has been investigated for hydrogen production in a fixed bed reactor. Experimental conditions include atmospheric pressure and temperature of 400-700°C. Catalyst used is nickel based and for CO₂ adsorption dolomite is used. The results show that

- With the increase in temperature hydrogen formation increases.
- Methane formation is negligible above 500°C.
- The optimum temperature for H₂ production for CO₂ adsorption using dolomite is 500°C.

Binlin Dou et al.[10] This paper involves the investigation of crude glycerol steam reforming reaction in a fixed bed reactor with and without CO₂ removal. Experimental conditions include temperature of 400°C to 700°C and atmospheric pressure. The process outputs were compared to those using pure glycerol. Results obtained for crude glycerol are compared with those obtained pure glycerol steam reforming. The results show that at 600°C glycerol conversion of 100%, steam conversion of 11% and hydrogen purity of 68% can be obtained. Also, Steam reforming with CO₂ adsorption can be effective and can achieve H₂ purity of 88%.

2.3 Modeling and simulation

The modeling and simulation of a fluidized bed reactor has been a difficult task and various authors have made attempts to do this in recent past. In this section a review of modeling and simulation work done is carried out.

Jamal Chaouki et al.[20]- In this work natural gas catalytic oxidation reaction for ethylene synthesis has been simulated in a turbulent fluidized bed reactor (TFBR) using a two phase model. The bed is filled with MgO catalyst particles. Probability distribution function of local voidage has been used to determine the distribution of primary and secondary phase. The mean voidage for emulsion phase and bubble phase increased with increase in gas superficial velocity. The results obtained from two phase model developed showed considerable agreement with the experimental values and thus it can be used for modeling of catalytic oxidation of natural gas for ethylene synthesis in a turbulent fluidized bed reactor.

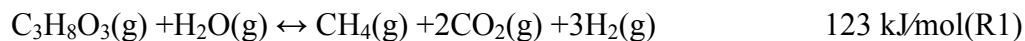
L.M Zou et al.[21] In this work gas-solid fast fluidized bed is simulated using a Eulerian-lagrangian approach. The lagrange approach treats the secondary phase as a discrete phase and each particle is tracked using equation of motion. The author has developed the cluster based drag coefficient model. This model uses a hydrodynamic equivalent diameter to calculate the Re for the secondary phase. The results obtained through simulation of fast fluidized bed using cluster based model are in good agreement with the experimental results. Also, the results obtained by using cluster based model are more accurate than those predicted by Wen and Yu drag model.

Paola Lettieri et al.[22] In this work commercial simulation software CFX4.4 has been used to simulate a liquid-solid fluidized bed having lead shots in slugging mode. The two dimensional geometry is created and time dependent simulations have been carried out. Already in built kinetic model for granular flow in CFX4.4 has been used for the simulation. The analysis has been done regarding all the aspects of fluidized bed viz. pressure drop, voidage profiles and slug formation. The results show that the pressure drop across the fluidized bed is greater than the theoretical value and which is in good agreement with the experimental values.

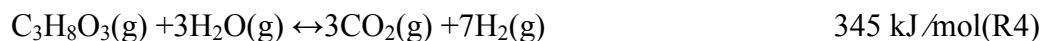
S. Benyahia et al.[23] In this work simulation software Fluent has been used to carry out the simulation for riser section of circulating fluidized bed reactor. The solid phase is the fluidized catalytic cracking (FCC) particles while the gas phase used is air. A two dimensional (2-D) time dependent isothermal flow is simulated for continuous gas phase and dispersed solid phase. Fluent solves the conservation equations for mass and energy using the finite volume approach. The results included the analysis of bed in terms of voidage and pressure drop profiles. Also, the computational values were in good agreement with the experimental values.

Jack T. Cornelissen et al. [24] In this work a liquid-solid fluidized bed is simulated using a multi-fluid computational fluid dynamics (CFD) model. The results show that CFD model prediction are in good agreement with the experimental results available in the literature. Varying the coefficient of restitution does not vary the results. Gidaspow and Wen Yu drag model are used and Gidaspow predicting the higher voidage. Also, two different liquid distributors uniform and non-uniform are simulated. It is concluded that better representation of distributor geometry did not alter the results that much.

Binlin Dou et al.[11] In this work glycerol steam reforming reaction in a fluidized bed reactor has been simulated using a commercial simulation software Fluent. The Eulerian –Eulerian two fluid approach model available in fluent is used to simulate the reactor. Reactions are incorporated as a three ate reaction mechanism through laminar finite rate modeling. At temperature at 600⁰C coke formation during the reaction is not considered thus simplifying the model. The model included the following reactions to examine the fluidized bed reaction kinetics:



The overall reaction of hydrogen production from glycerol steam reform can be written as:



The results show that reactor is heterogeneous in nature. Clusters of solid phase are observed to form in the reactor Thus proper stirring is required to maintain the fluidization condition. The glycerol conversion increased with flow time and most of the product gases are formed within first 2 seconds. Steady state is found to be achieved after 4 seconds. The results obtained through this gas-solid fluidized bed simulation will provide useful to design the industrial catalytic fluidized bed reactor.

Sebastian Zimmermann et al.[16] In this work, a gas-solid fluidized bed with fluidized catalytic cracking (FCC) particles is simulated using a commercial computational fluid dynamics CFD solver FLUENT. Ozone decomposition reaction is simulated in the reactor. Two drag models Gidaspow and Syamlal and O'Brien are used in the simulation but both overestimated the bed expansion than the results obtained from experiments. Thus modified Syamlal O'Brien drag model which is based on the minimum fluidization conditions is used which correctly predicted the bed expansion.

Ozone decomposition reaction is included by incorporating an additional transport equation with a kinetic term in the model. The results show that the conversion predicted for ozone is higher than the experimental data which can be attributed to the effect of gas distributor (not considered in CFD simulation). The reaction kinetics for ozone decomposition was included in the CFD model to evaluate the predictions of the fluidized-bed reactor kinetics. Ozone decomposition follows first-order reaction kinetics.

3 CFD Modeling of fluidized bed reactor

Fluidized beds are widely used in chemical, petrochemical, metallurgical and other industries. Major applications are Fluidized catalytic cracking (FCC) and bubbling fluidized bed (BFB) combustor of gasifier systems. Although Fluidized beds are widely used in industrial applications but much research has to be done in order to understand and predict the hydrodynamics of the reactor. Hydrodynamics majorly affect the efficiency of such reactors. With the advancement of computational fluid dynamics (CFD) we now have a tool to simulate the fluidized bed. User friendly CFD packages are available for research and commercial purposes.

3.1 Approaches to Gas-Solid Fluidization Modeling

Gas-solid fluidized bed can be modeled in two ways which depend on the way the solid phase is treated in simulation. One is the Eulerian-Eulerian approach or two fluid model (TFM) in which gas phase and solid phase both are treated as a continuous media. Other one is Eulerian - Lagrangian approach or discrete element method (DEM) in which solid particles are treated as discrete particles and gas is considered as continuous phase.

In Eulerian-Lagrangian approach solid phase is treated at the particle level (point mass representation). In point mass representation the particles are much smaller than grid spacing and it does not affect the gas domain or its discretization. The trajectory of these solid particles in gas phase is determined by integration of particle equation of motion (PEM) which takes into account the forces acting on the particle.

In Eulerian-Eulerian approach both the solid phase and the gas phase are considered as continuum and both phase as interpenetrating continuum. Since solid phase are also considered as continuum thus additional closure laws are also required to describe the rheology of the particles. The Eulerian approach has several advantages over the Lagrangian approach:

- Less computational expensive for the same type of problem.
- Computational requirement does not change much on addition of few more solid particles.

3.2 Computational flow model

The Eulerian-Eulerian two fluid model is used to model the glycerol steam reforming reactor. The chemical reactions are modeled using laminar finite rate model. The granular properties of solids in the bed are predicted using kinetic theory of granular flow. Ansys fluent 13 is used to carry out the modeling and simulation.

3.2.1 Gas-solid flow equations

The prediction for gas-solid flow pattern in the riser of a fluidized bed is achieved by numerical solution of the mass and momentum conservation equations for both the phases

Continuity equation

The volume fraction for each phase is calculated with the use of continuity equation for each phase. The continuity equation for phase q is

$$\frac{\partial(\rho_q \varepsilon_q)}{\partial t} + \nabla \cdot (\rho_q \varepsilon_q v_q) = 0 \quad (3.1)$$

Where q=g for gas phase and s for solid phase, v is the velocity vector, and ρ is the density, ε is the fraction of each phases with the constraint:

$$\sum \varepsilon_q = 1 \quad (3.2)$$

Momentum equations

The gas phase momentum conservation equation:

$$\frac{\partial(\rho_q \varepsilon_q v_q)}{\partial t} + \nabla \cdot (\rho_q \varepsilon_q v_q v_q) = -\varepsilon_q \nabla p + \nabla \tau_g - K_{gs}(v_g - v_s) + \rho_q \varepsilon_q g \quad (3.3)$$

$$\tau_g = \varepsilon_q \mu_g (\nabla v_g + \nabla v_g^T) \quad (3.4)$$

The solid phase momentum conservation equation:

$$\frac{\partial(\rho_s \varepsilon_s v_s)}{\partial t} + \nabla \cdot (\rho_s \varepsilon_s v_s v_s) = -\varepsilon_s \nabla p + \nabla p_s + \nabla \tau_s - K_{gs}(v_s - v_g) + \rho_s \varepsilon_s g \quad (3.5)$$

$$\tau_s = 2\varepsilon_s \mu_s (\nabla v_s + \nabla v_s^T) + \varepsilon_s (\lambda_s - \frac{2}{3} \mu_s) \nabla v_s \bar{I} \quad (3.6)$$

Properties model equations

To describe the behavior of solid particles in fluidized bed the properties model for interaction with the gas and other solids is to be defined.

Granular viscosity

The Granular viscosity is a summation of three viscosities which are collisional, kinetic and frictional viscosity.

$$\mu_s = \mu_{s,col} + \mu_{s,kin} + \mu_{s,fr} \quad (3.7)$$

$\mu_{s,col}$ = collisional viscosity which is due to the collision between the particles which is taken from kinetic theory of granular flow of Lun et al and can be represented as represented as

$$\mu_{s,col} = \frac{4}{5} \varepsilon_s \rho_s d_s (1 + e) g_0 \left(\frac{\theta_s}{\pi} \right)^{1/2} \quad (3.8)$$

where, g_0 is the radial distribution function, e is the restitution coefficient and θ_s is the granular temperature.

$\mu_{s,kin}$ = kinetic viscosity from Gidaspow et al model

$$\mu_{s,kin} = \frac{2\mu_{s,dil}}{(1+e)g_0} \left[1 + \frac{4}{5} g_0 \varepsilon_s (1 + e) \right]^2 \quad (3.9)$$

The solid phase dilute viscosity in above equation is expressed by:

$$\mu_{s,dil} = \frac{5\rho_s d_s \sqrt{\theta_s \pi}}{96} \quad (3.10)$$

$\mu_{s,fr}$ = frictional viscosity which is the contribution of the friction between the particles to the total shear viscosity. when the solids are very close to each other the main stress will be due to friction and rubbing between the particles. Schaeffer expression for the frictional viscosity is used for this equation.

$$\mu_{s,fr} = \frac{P_{s,fr} \sin \varphi}{2\sqrt{I_{2D}}} \quad (3.11)$$

Where $P_{s,fr}$ is the frictional pressure, φ is the angle of internal friction and I_{2D} is the second invariant of the deviatoric stress tensor.

Granular bulk viscosity

The granular bulk viscosity is the resistance the granular particles offer to compression and expansion. The expression is taken from Lun et al and is developed on the basis of kinetic theory of granular flow.

$$\lambda_s = \frac{4}{3} \varepsilon_s \rho_s d_s g_0 (1 + e) \left(\frac{\Theta_s}{\pi} \right)^{\frac{1}{2}} \quad (3.12)$$

Granular conductivity

The granular conductivity describes the diffusive flux of granular energy or granular temperature. The expression is taken from Gidaspow et al.

The diffusion coefficient for granular energy (k_s) is expressed as:

$$k_s = \frac{150 \rho_s d_s \sqrt{\Theta_s \pi}}{384(1+e)g_0} \left[1 + \frac{6}{5} \varepsilon_s g_0 (1 + e) \right]^2 + 2 \varepsilon_s \rho_s d_s g_0 (1 + e) \left(\frac{\Theta_s}{\pi} \right)^{1/2} \quad (3.13)$$

Solids Pressure

The solid pressure term contain a collision term and kinetic term. The solid pressure is highest when the bed is not fluidized. It decreases to a minimum value when fluidization starts and again increases after that due to particle collisions.

Solid pressure(p_s) is expressed as (Lunet al model):

$$p_s = \rho_s \varepsilon_s \Theta_s [1 + 2(1 + e) \varepsilon_s g_0] \quad (3.14)$$

where e is the restitution coefficient, and g_0 is the radial distribution function.

Radial distribution function

Radial distribution function (g_0) is the factor that modifies the probability of collision between particles. It can be seen as the distance between the solids particles.

$$g_0 = \frac{s+d_p}{s} \quad (3.15)$$

where s is the distance between the spheres. It can be seen from above equation that as s tends to infinite then g_0 tends to one and when s tends to zero g_0 tends to infinite.

Radial distribution function can be expressed as:

$$g_0 = \frac{3}{5} \left[1 - \left(\frac{\varepsilon_s}{\varepsilon_{s,max}} \right)^{\frac{1}{3}} \right]^{-1} \quad (3.16)$$

$\varepsilon_{s,max}$ is the particle volume fraction at maximum packing.

Granular temperature

The granular temperature of solid phase depicts the kinetic energy of random motion of particles. Random motion of particles is due to mechanical energy transferred to the particles. If the collisions are perfect than all the kinetic energy is conserved but in reality collision is not perfect thus there is increase in the temperature of particles.

The conservation of the kinetic energy is shown below:

$$\frac{3}{2} \left[\frac{\partial(\rho_s \varepsilon_s \Theta_s)}{\partial t} + \nabla \cdot (\rho_s \varepsilon_s v_s \Theta_s) \right] = (p_s \bar{I} + \tau_s) : \nabla v_s + \nabla \cdot (k_s \nabla \Theta_s) - \gamma_s + \varphi_{gs} \quad (3.17)$$

Where Θ_s : is granular temperature.

The diffusion coefficient for granular energy (k_s) is expressed by the Gidaspow model:

$$k_s = \frac{150 \rho_s d_s \sqrt{\Theta_s \pi}}{384(1+e)g_0} \left[1 + \frac{6}{5} \varepsilon_s g_0 (1+e) \right]^2 + 2 \varepsilon_s \rho_s d_s g_0 (1+e) \left(\frac{\Theta_s}{\pi} \right)^{\frac{1}{2}} \quad (3.18)$$

The collision dissipation of energy (γ_s) is calculated from:

$$\gamma_s = \frac{12(1 - e^2)g_0}{d_s\sqrt{\pi}} \varepsilon_s \rho_s \Theta_s \quad (3.19)$$

The kinetic energy transfer function (φ_{gs}) is expressed as:

$$\varphi_{gs} = -3K_{gs}\Theta_s \quad (3.20)$$

Drag models

The drag models describe the momentum exchange between the particles. The expression used for solid-fluid exchange coefficient is given by Gidaspow et al. Gidaspow drag model is combination of two drag models one for dense regime and the other for dilute regime. For $\alpha_g \leq 0.8$ Ergun equation for pressure drop calculation in packed bed is used and for $\alpha_g > 0.8$ Wen and Yu model is used.

If $\varepsilon_g > 0.8$, then K_{gs} is calculated with the equation from the Wen and Yu model as

$$K_{gs} = \frac{3}{4} C_D \frac{\varepsilon_s \rho_g \varepsilon_g |\vec{v}_s - \vec{v}_g|}{d_s} \varepsilon_g^{-2.65} \quad (3.21)$$

Where C_D is the drag coefficient

$$C_D = \begin{cases} \frac{24}{Re} (1 + 0.15Re^{0.687}), & Re < 1000 \\ 0.44, & Re \geq 1000 \end{cases} \quad (3.22)$$

and the Re is calculated as follows:

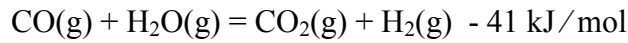
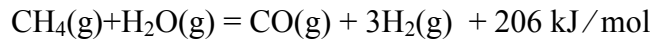
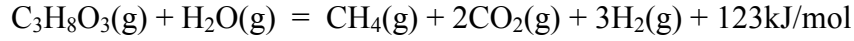
$$Re = \frac{\rho_g d_s |\vec{v}_s - \vec{v}_g|}{\mu_g} \quad (3.23)$$

If $\varepsilon_g \leq 0.8$, then K_{gs} is calculated with the dense phase model of the Ergun equation which is given as :

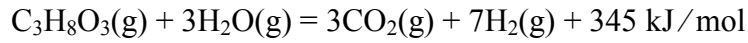
$$K_{gs} = 150 \frac{\varepsilon_s \varepsilon_s \mu_g}{\varepsilon_g d_s d_s} + 1.75 \frac{\varepsilon_s \rho_g |\vec{v}_s - \vec{v}_g|}{d_s} \quad (3.24)$$

3.2.2 Reaction model

The Glycerol steam reforming is a complex set of reactions whose pathway depends on catalyst and reaction condition. The intermediate product methane undergoes steam reforming reactions thus producing hydrogen, carbon mono-oxide and carbon di-oxide. In previous study it is indicated that quantity of coke formed is negligible at temperature above 600°C. Thus in this simulation includes following reactions.



The overall reaction of hydrogen production from glycerol steam reforming can be written as:



All three reactions are considered to be first order and modeled through laminar finite rate model. Reaction kinetics of all the reactions are expressed by Arrhenius expression. Reactions takes place in the entire riser section and following transport equation is gives the mole fraction of each species, X_i .

$$\frac{\partial(\rho_i X_i)}{\partial t} + \nabla \cdot (\rho_i \vec{v}_i X_i) = -\nabla J_i + R_i \quad (3.25)$$

where J_i , the rate of diffusion of species i , is expressed as:

$$J_i = -\rho_i D_i \nabla X_i \quad (3.26)$$

R_i is the source term (rate of formation) for species i which is calculated as the sum of the species sources in all the reactions in which the species participates.

4 Solution Methodology

4.1 Problem statement

The simulation of glycerol steam reforming in a bubbling fluidized bed reactor has to be done with help of CFD technique using a Fluent software (Ansys 13). The reactor is of 1m height and 0.3m width. Reactor is initially filled with solid catalyst bed up to a height of 0.12m and solid volume fraction of 0.52. The solid bed is made up of Ni/Al₂O₃ catalyst which is fluidized by mixture of gases coming from the bottom of the bed. Gaseous mixture has glycerol, steam and nitrogen (which is used as a inert gas). Reactor is maintained at isothermal conditions (constant temperature) of 600⁰C. Outlet pressure is defined to be atmospheric pressure. Glycerol steam reforming reactions occurs in the reactor in the presence of catalyst thus producing a mixture of gases containing H₂, CO, CO₂, CH₄ and inert N₂ at the outlet. Figure 1 represents the experimental set up and Table 1 gives the parameters values available to us.

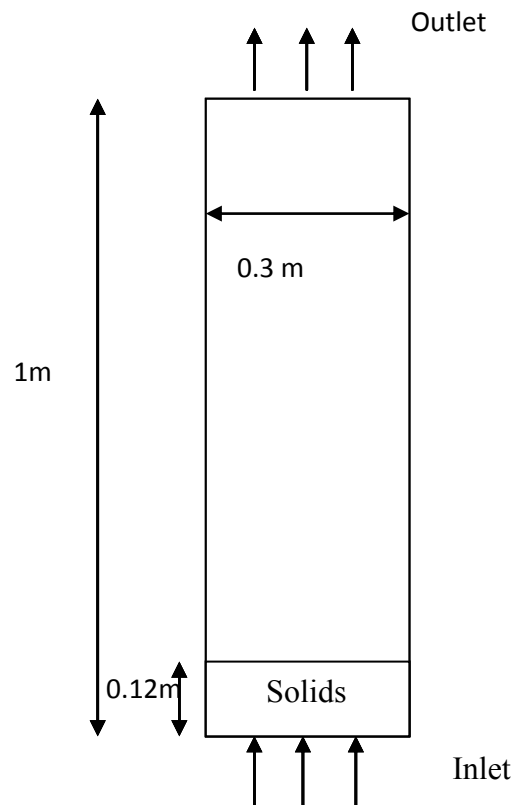


Figure 4.1: Reactor set up

Table 4.1: Glycerol steam reforming reactor set up

Reactor set up	Value
Height	1m
width	0.3m
temperature	600 ⁰ C
Gas phase	Value
Inlet molar flow rate of components	
Glycerol	1.1x10 ⁻³ kmol/m ³
Steam	6.22x10 ⁻³ kmol/m ³
Nitrogen	3.24x10 ⁻² kmol/m ³
Inlet gas velocity	0.5 m/s
Solid phase	Value
Size (diameter) and shape	8.75x10 ⁻⁵ m, spherical
Density	2650 kg/m ³
Initial bed height	0.12m
Initial void fraction	0.52

4.2 Numerical Methodology

In order to do simulations of glycerol steam reforming in fluidized bed reactor (described in the problem statement chapter) Eulerian -Eulerian two fluid approach with laminar finite rate modeling for reactions is used. Equations describing Eulerian -Eulerian approach and laminar finite rate model are mentioned in CFD modeling chapter.

Geometry and grid

Grid was created for fluidized bed of dimensions 1m tall and 0.3m in width in CAD program called GAMBIT. Then grid is exported to simulation software called ANSYS FLUENT 13. Fig 4.2 shows the two dimensional grid of the reactor and the initial solid bed height patched with initial solid volume fraction .

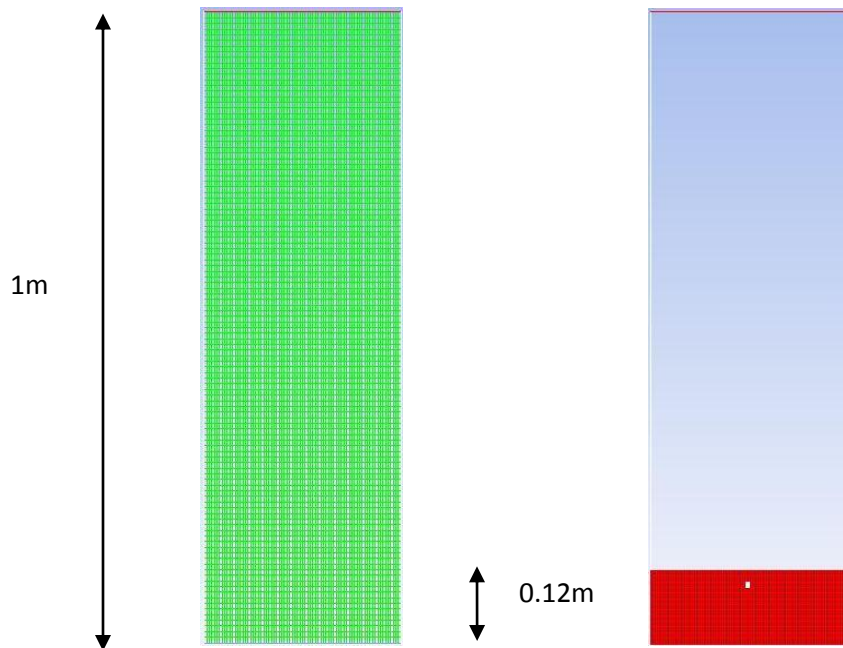


Figure 4.2: Grid and patch field.

Simulation set up

The gas phase is isothermal mixture containing a mixture glycerol, steam and N₂. As there is low pressure in the system gas is assumed to be incompressible. The particulate phase is assumed to have single density and single size of particles. Initial particle normal velocity is set to zero. The setup for other properties of the secondary phase and primary phase are given in the following table.

The governing equations for laminar flow of gas are solved by finite volume approach. Second order upward discretization scheme for the convection terms are used. The reactions are described by first order reaction kinetics with kinetics parameters taken from literature and given in the following table.

Table 4.2: 2D grid of the reactor

No. of cells	8512
No. of faces	17212
No. of nodes	8701
Cells	Quadrilateral

Table 4.3: Operating and boundary conditions

Inlet boundary condition	Velocity inlet
Outlet boundary condition	Pressure outlet
Wall boundary condition	No slip
Acceleration due to gravity	-9.81m/s ²
Operating pressure	1 atm

Table 4.4: Simulation set up

Time step size	0.001s
Convergence criteria	10^{-4}
Discretization method	Second order upwind
Drag law	Gidaspow
Coefficient of restitution	0.95
Granular bulk viscosity	Lun-et al.
Granular conductivity	Gidaspow et al.
Solid pressure	Lun-et al

Table 4.5: Values of kinetic parameters for reactions.

Reaction	k value
$C_3H_8O_3(g) + H_2O(g) = CH_4(g) + 2CO_2(g) + 3H_2(g)$	$1.838 \times 10^8 \exp(-74210/RT)$
$CH_4(g) + H_2O(g) = CO(g) + 3H_2(g)$	$5.933 \times 10^8 \exp(-209200/RT)$
$CO(g) + H_2O(g) = CO_2(g) + H_2(g)$	$6.028 \times 10^{-4} \exp(-15400/RT)$

5 Results and Discussions

The model equations given in chapter 3 for gas-solid fluidized bed reactor have been solved using the commercial simulation software FLUENT 13.0 (ANSYS). In this section the simulation results obtained are presented.

5.1 Hydrodynamics of fluidized bed

The hydrodynamics of fluidized bed includes the solid-gas interaction within the reactor. The analysis includes the investigation of pressure drop, distribution of solid and gas phase in the reactor. Following section gives the simulated results regarding the hydrodynamics of bed.

5.1.1 Pressure drop across the bed

The pressure drop in the fluidized bed does not theoretically vary with time after the minimum fluidization condition. The pressure drop is equal to the weight of solids in the bed. But in actual there is continuous variation in pressure drop this can be attributed to the gas-solid phase interaction and fluidization conditions.

An expression of pressure drop across the bed can be given as:

$$\Delta P = (\rho_s - \rho_g)(1 - \epsilon_{mf})gL \quad (5.1)$$

Where, L is the bed height,

ϵ_{mf} is the minimum fluidization condition bed void fraction,

ρ_s and ρ_g are the solid and gas phase density.

Fig 5.1 shows the pressure drop variation with flow time in the fluidized bed reactor. The straight horizontal line is for theoretical pressure drop and the blue line is the simulated results. The porosity at minimum fluidization condition can be determined experimentally, and it is given to be 0.5. Theoretical value of pressure drop from equation 5.1 comes to be 1560 Pa.

$$\Delta P = (1-0.5)*9.81*2650*0.12=1560 \text{ Pa}$$

From the figure 5-1 it can be seen there is considerable fluctuation in pressure drop across the bed with flow time. However after 2 sec the theoretical and the simulated value are very close. Fluctuation in pressure drop in the reactor can be attributed to the unsteady state before 2 sec and clusters form of solid phase in the reactor. The prediction of pressure drop in fluidized bed has been a problem in industries.

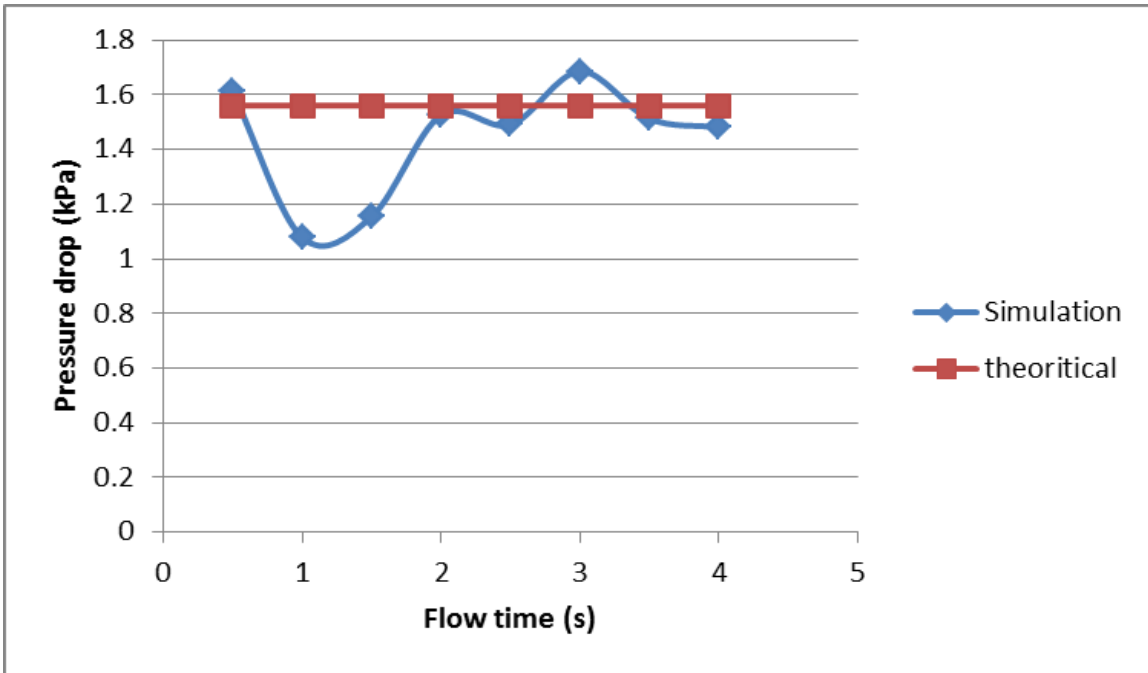
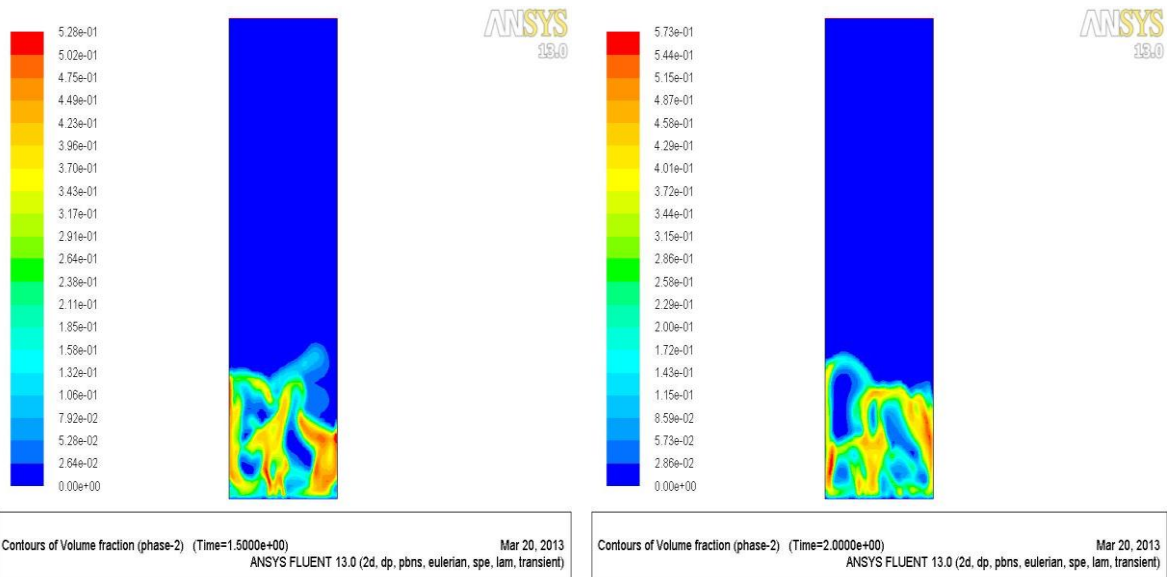
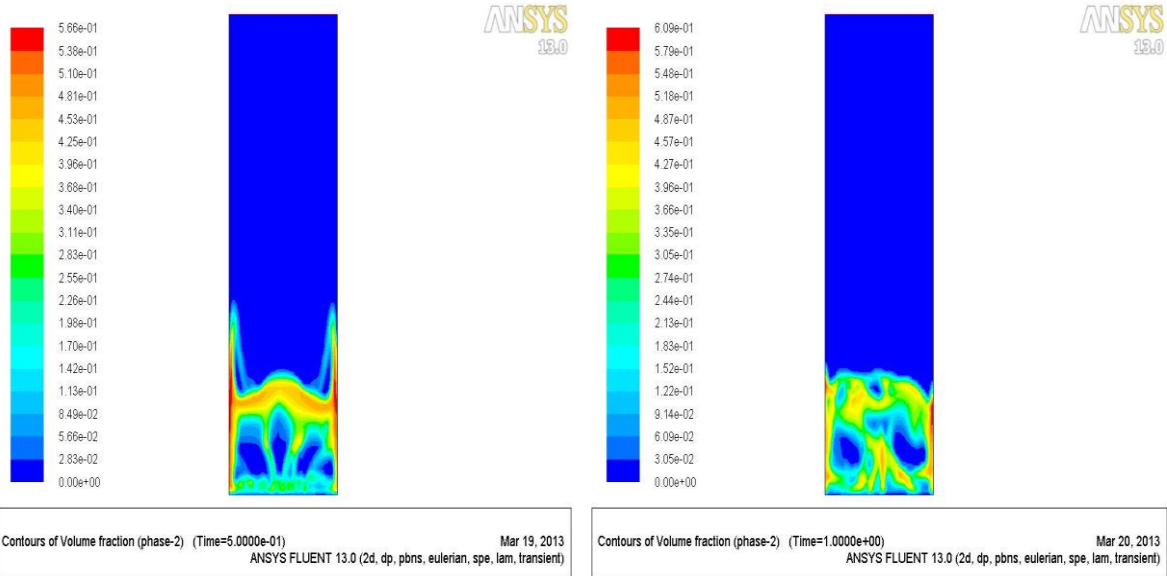


Figure 5.1: Pressure drop variation with flow time.

5.1.2 Contours of volume fraction of solid phase in reactor

The contours of solid phase in reactor help to analyze the distribution of gas and solid phase in the reactor. Figure 5-2 gives the contours of solid phase inside the reactor using Gidaspow drag model at different flow time. It is clear from the graphs clusters are formed in the reactor thus giving reactor heterogeneous nature.



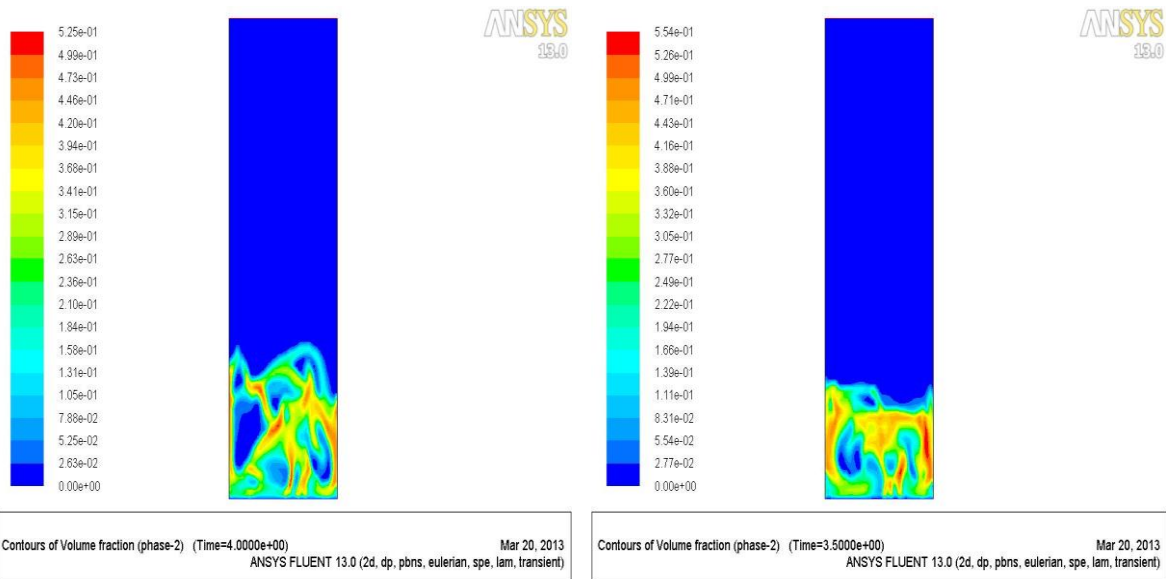
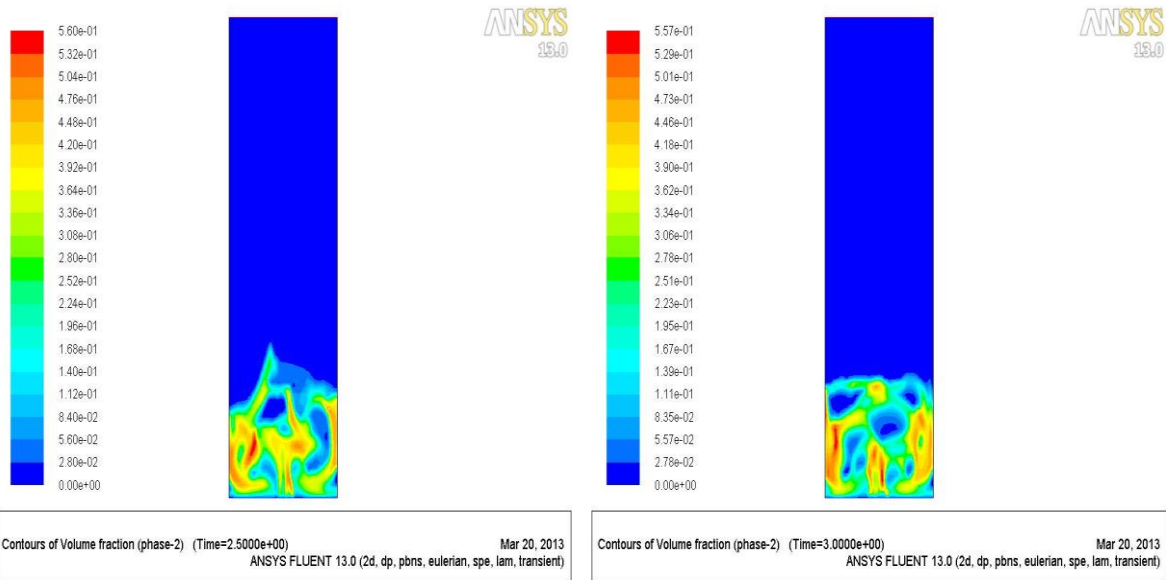


Figure 5.2: Contours of solid volume fraction with flow time.

5.2 Reactant conversion and product yield

In order to depict the glycerol steam reforming reaction in the simulation three-reactions are included in reaction mechanism of the model. Reactions are of first order with respect to both steam and glycerol and without considering the reverse reaction as the effect of reverse reaction on hydrogen production by glycerol steam reforming is negligible at temperature above 600⁰C. In order to simplify the model coke formation is neglected as available in some literature. Reactor performance is determined by measuring the glycerol, steam conversions and product formation.

In the reactor reactants glycerol and steam are converted to gaseous products which are hydrogen, carbon dioxide, carbon mono-oxide and methane. The outlet stream consists of product gases, unconverted glycerol, steam and inert gas nitrogen used in the reactor.

5.2.1 Glycerol and steam conversion

Glycerol and steam conversion can be calculated as:

$$Conv_i = 100 X \frac{(N_i X_i v_i)_{inlet} - \sum_1^{N_k} (X_i v_i)_{outlet}}{(N_i X_i v_i)_{inlet}}$$

Where,

N_k is the cell number at inlet, and

x_i represents the molar fraction of species i , and i represents the reactants.

Figure 5-3 shows the glycerol and steam conversion with flow time. It can be observed glycerol conversion increases with flow time and reaching a value of 45% at 4 second, and then reaches a steady state condition. Steam conversion was in the 15 % range after 2 second .

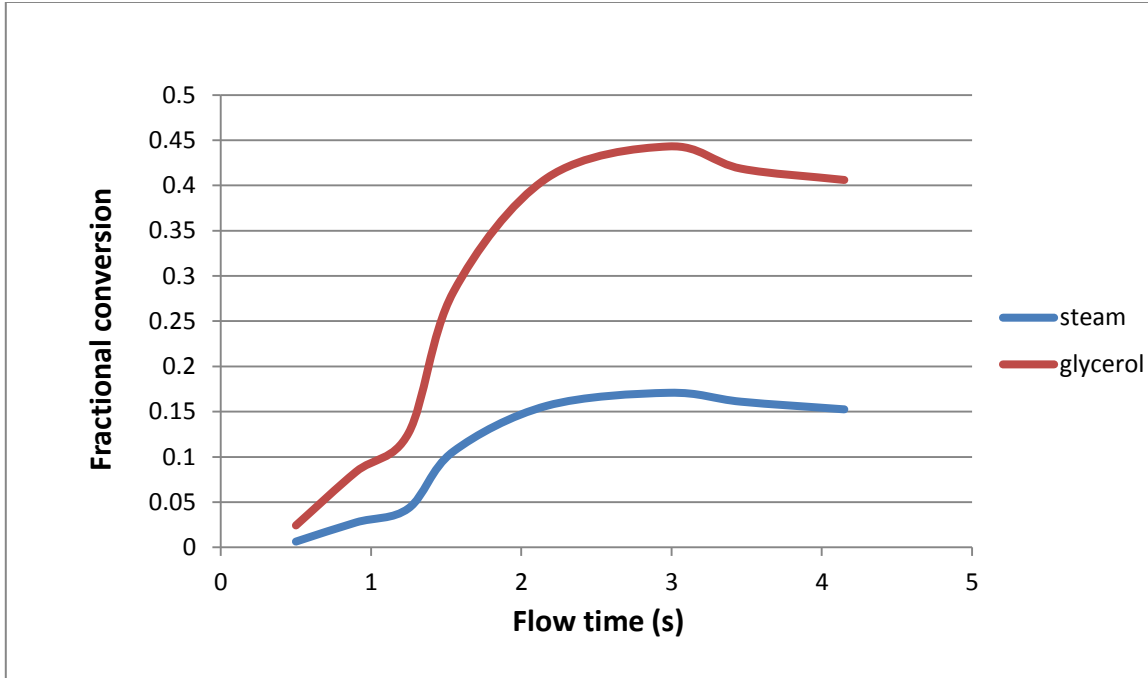


Figure 5.3: Fractional conversion of glycerol and steam with flow time.

5.2.2 Product formation

Products of glycerol steam reforming reaction include H₂, CO₂, CH₄, CO gases. The average concentration of product species can be calculated in the outlet by :

$$Products_i = \frac{\sum_1^{N_k} (x_i v_i)}{\sum_1^{N_k} v_i}$$

Where,

x_i = is the mole fraction and v_i is the velocity of species.

Concentration in outlet of products (CH₄, H₂, CO₂, CO) in kmol/m³ v/s flow time is shown in figure 5-4. Most gas products are formed during the initial 2 s. The carbon mono-oxide concentration is much less than the other gases thus it is shown in different figure 5-5.

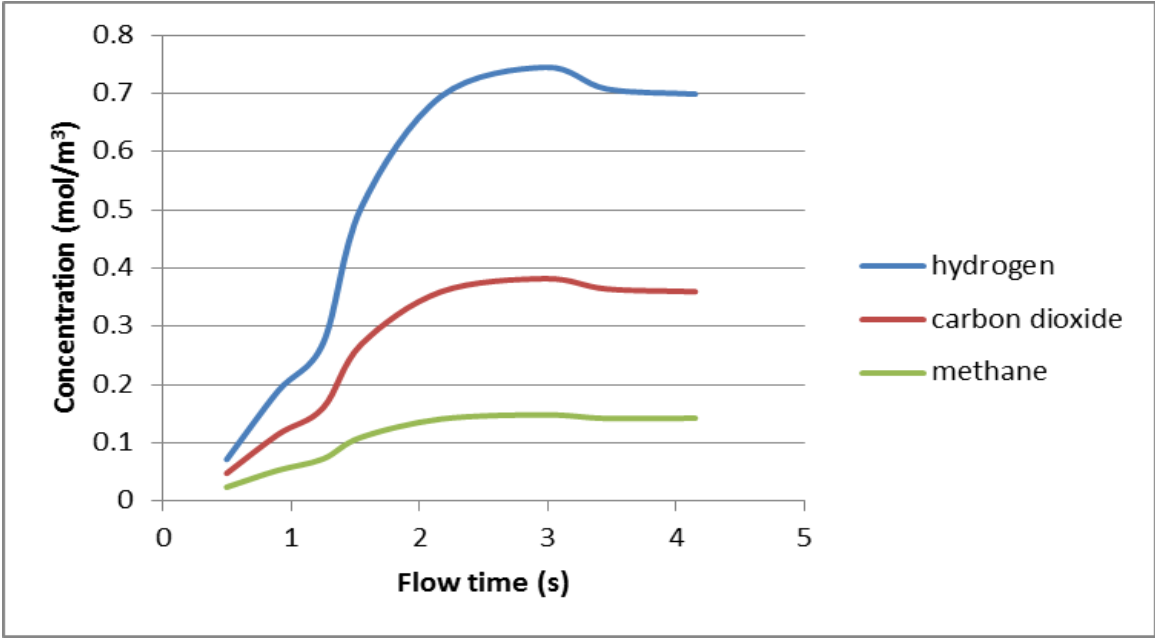


Figure 5.4: Concentration of product gases in outlet.

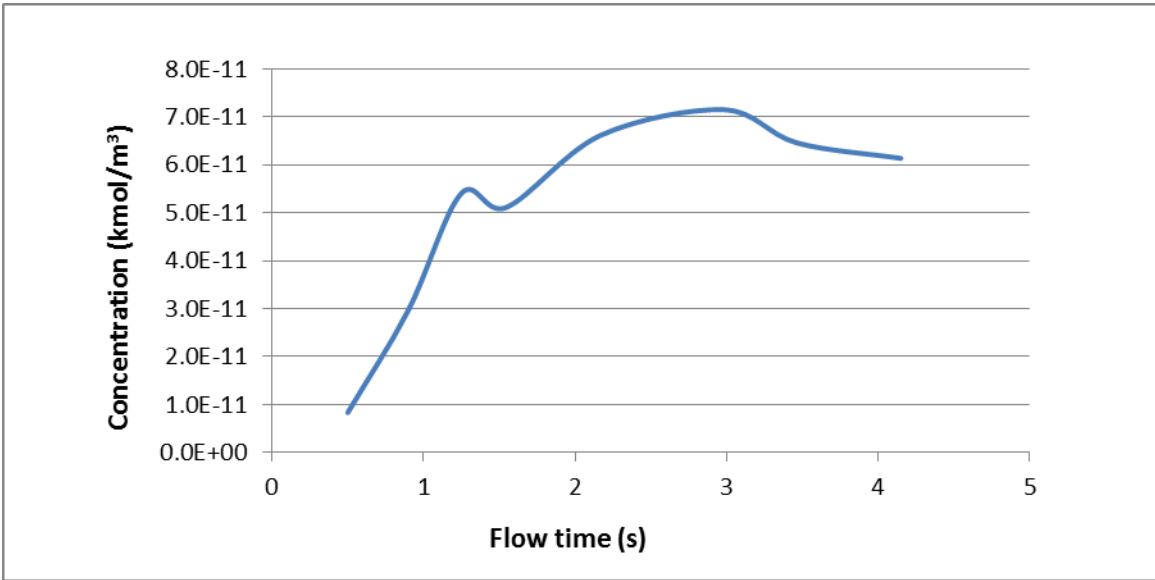


Figure 5.5: Concentration of CO in outlet.

Validation of model

The results obtained through simulation of glycerol steam reforming reaction in a fluidized bed reactor were in good agreement with the results obtained by author in "Computational Fluid Dynamics Simulation of Gas-Solid Flow during Steam Reforming of Glycerol in a Fluidized Bed Reactor" Energy & Fuels 2008, 22, 4102–4108.

The deviation of the simulated results from the experimental value for H₂, CO₂, CH₄ are within 8% of the error limit.

Table 5.1: Comparison of experimental and simulated results

	Experimental	Simulations
Catalyst	Ni/Al ₂ O ₃	Ni/Al ₂ O ₃
Temperature	600 ⁰ C	600 ⁰ C
Steam to carbon ratio	2:1	2:1
Product gas composition		
H ₂ (vol%)	59.1	54.8
CO ₂ (vol%)	27.2	30.9
CH ₄ (vol%)	5.9	14.2
CO (vol%)	7.8	0

5.3 Effect of process variables

The process variables which effect the glycerol conversion and the volume fraction of product gases are steam to carbon ratio (s/c) in the feed stream, inlet mixture velocity, reactor temperature. In this section results obtained through simulation by varying these process variables are given.

5.3.1 Variation of inlet mixture velocity

Inlet mixture velocity is changed from 0.5 m/s to 0.6 m/s. Three values of velocity (0.50, 0.55, 0.60 m/s) has been used in the simulation to see the effect on hydrogen production and glycerol conversion. This effect of velocity on product formation and reactant conversion is investigated at steam to carbon ratio of 2:1 and at temperature of 600⁰C. For velocity 0.5 m/s fig. 5-6 shows the concentration of product gases in the outlet with flow time. The Maximum value of hydrogen concentration reached in outlet is 0.81 mol/m³ .Figure 5-7 shows the concentration of glycerol in outlet with flow time. Glycerol concentration decreases with flow time and reaching the concentration of 0.6mol/m³ at 4 second. Figure 5-8 shows the conversion of glycerol with flow time. Glycerol conversion increases with flow time and reaching a value of 0.47 at 4 second.

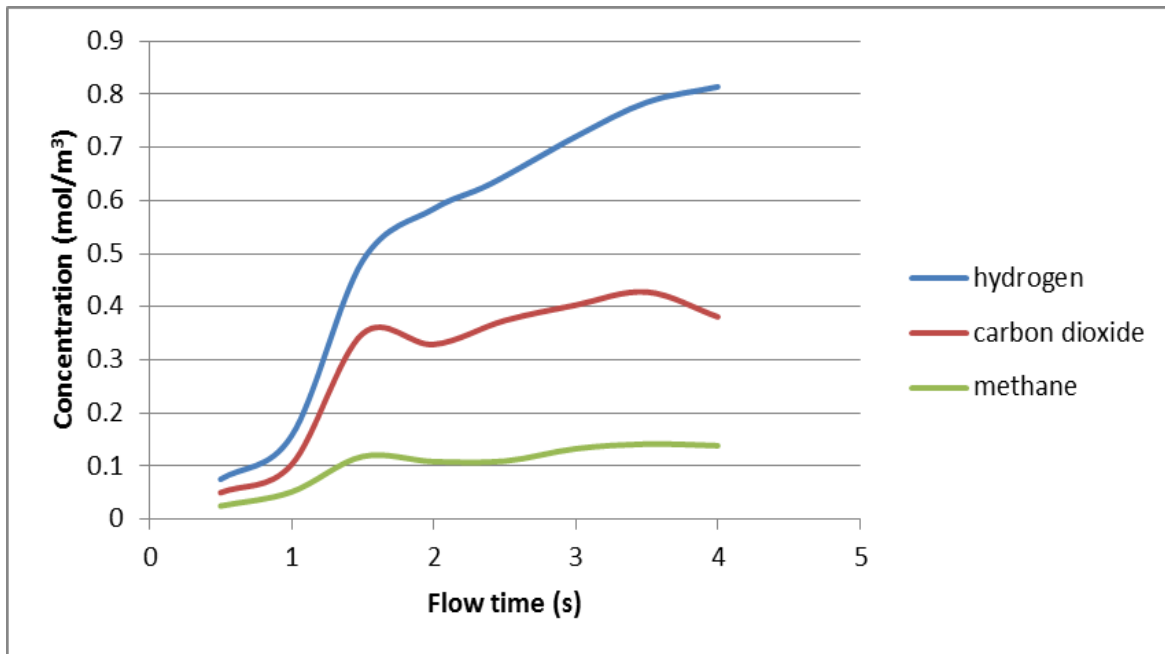


Figure 5.6: Product gas concentration with flow time (v=0.5m/s, s/c=2:1, T=600⁰C)

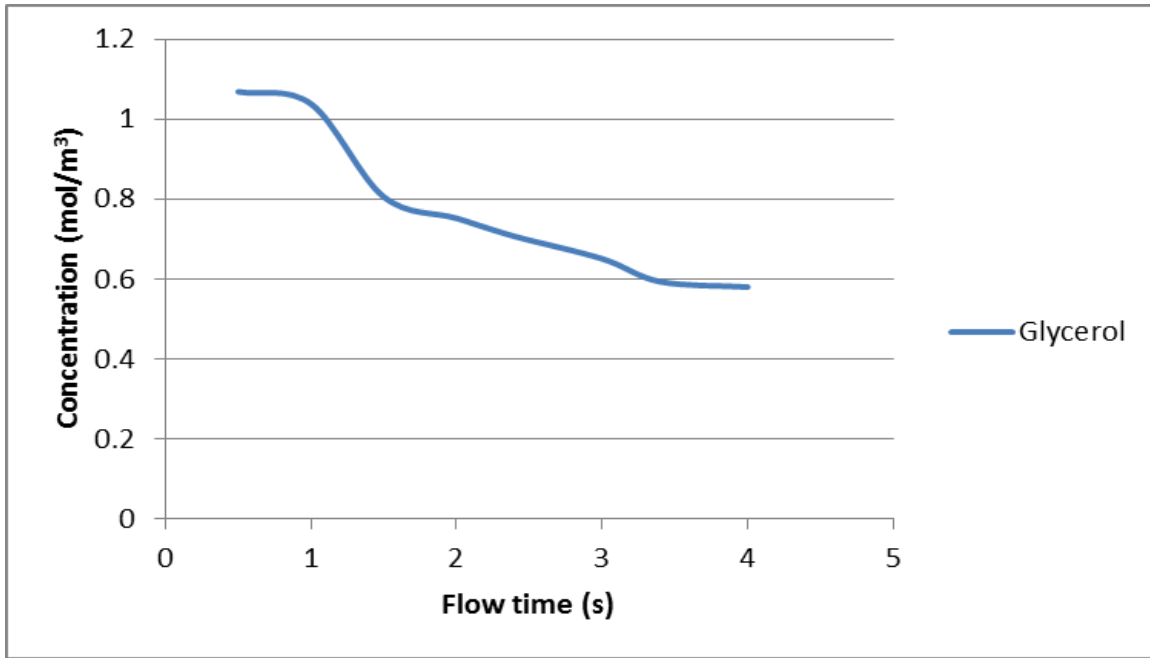


Figure 5.7: Glycerol concentration at outlet with flow time ($v=0.5\text{m/s}$, $s/c=2:1$, $T=600^{\circ}\text{C}$).

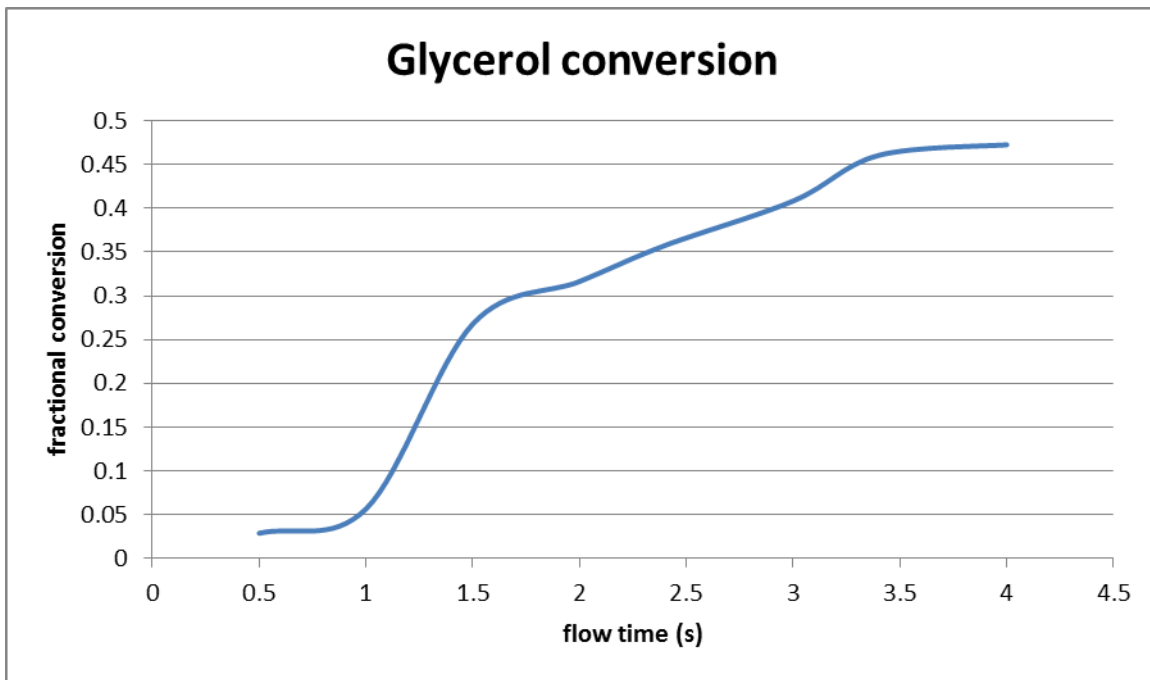


Figure 5.8: Glycerol conversion with flow time ($v=0.5\text{m/s}$, $s/c=2:1$, $T=600^{\circ}\text{C}$).

For velocity 0.55m/s , figure. 5-9 shows the concentration of product gases in the outlet with flow time. The Maximum value of hydrogen concentration reached in outlet is 0.73 mol/m^3 . Figure 5-10 shows the concentration of glycerol in outlet with flow time. Glycerol concentration decreases

with flow time and reaching the concentration of 0.64mol/m^3 at 4 second. Figure 5-11 shows the conversion of glycerol with flow time. Glycerol conversion increases with flow time and reaching a value of 0.42 at 4 second.

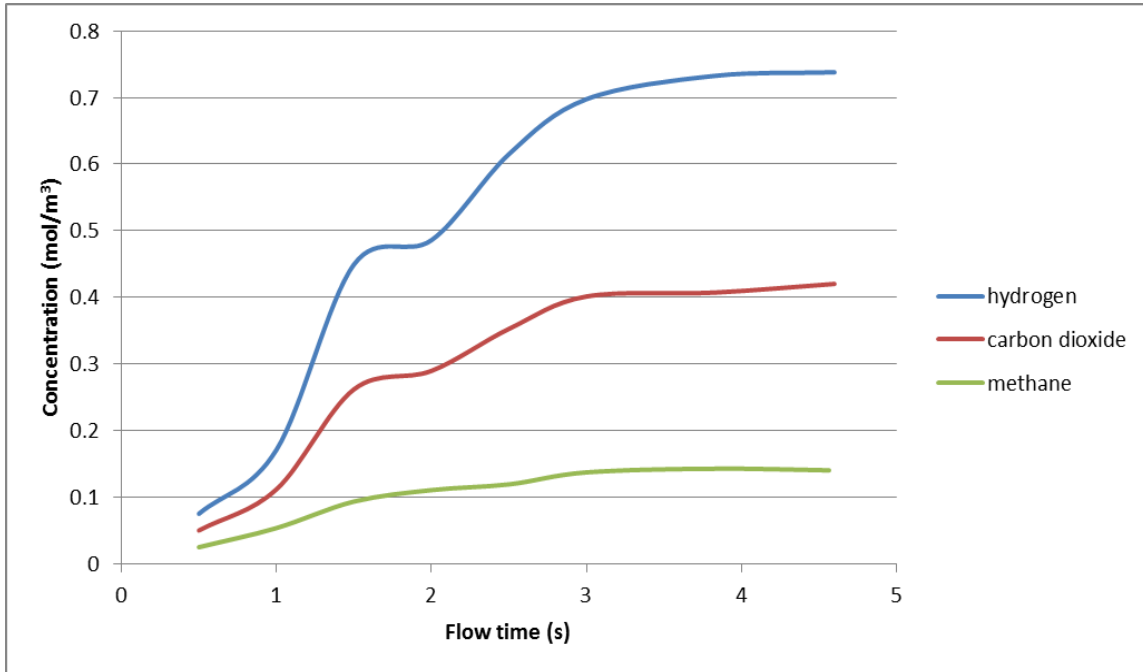


Figure 5.9: Product gases concentration with flow time ($v=0.55\text{m/s}$, $s/c=2:1$, $T=600^{\circ}\text{C}$).

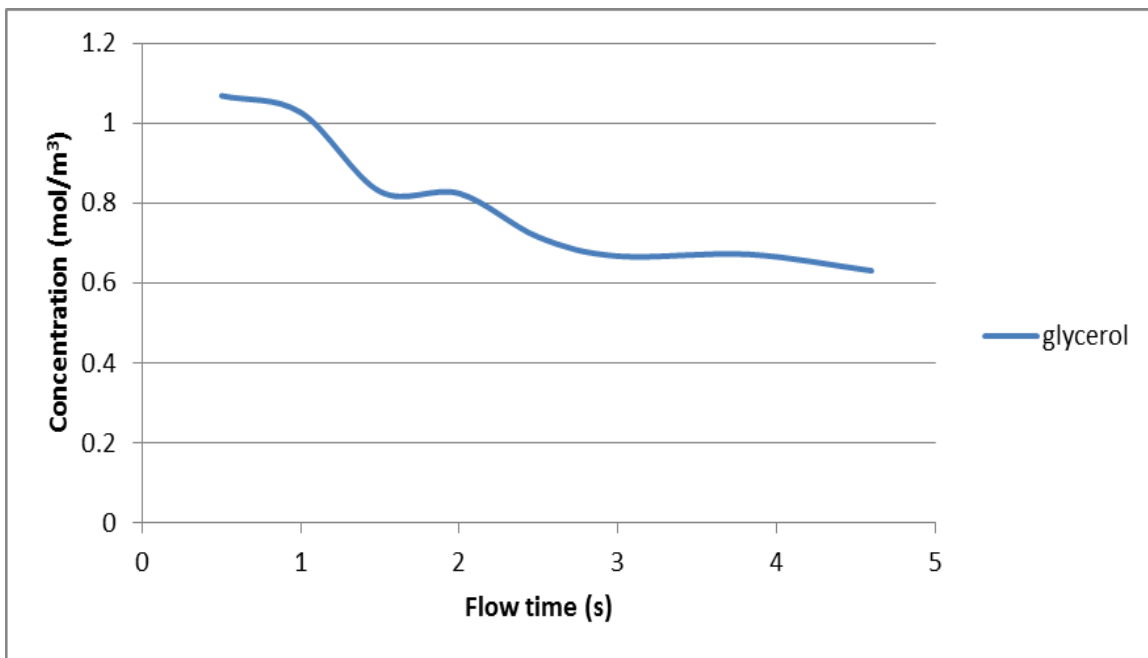


Figure 5.10: Glycerol concentration at outlet with flow time ($v=0.55\text{m/s}$, $s/c=2:1$, $T=600^{\circ}\text{C}$).

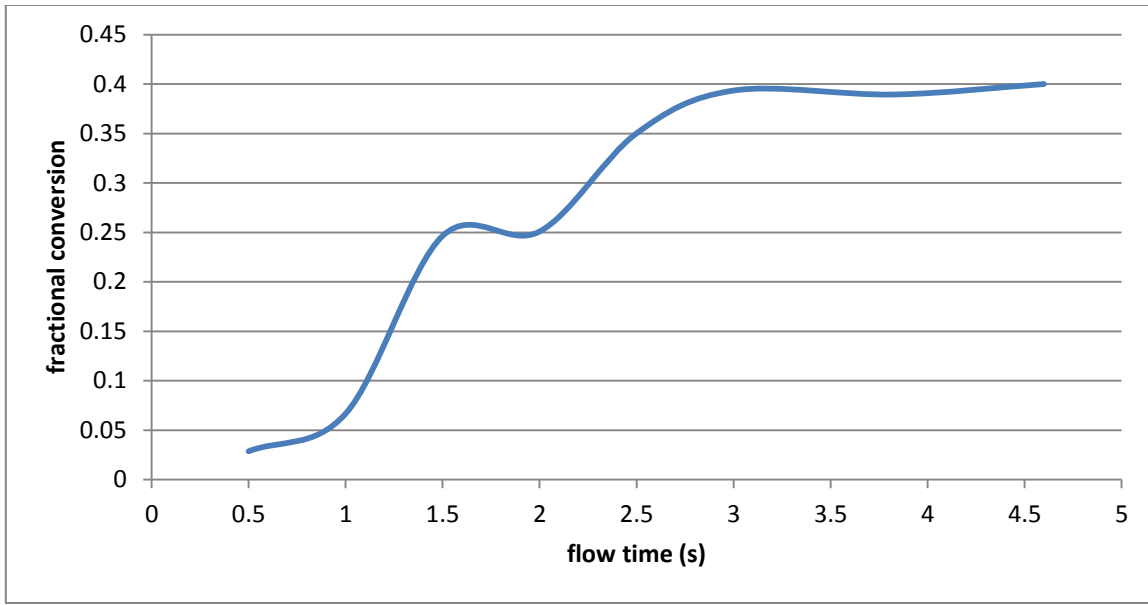


Figure 5.11: Glycerol conversion with flow time ($v=0.55\text{m/s}$, $s/c=2:1$, $T=600^{\circ}\text{C}$).

For velocity 0.6 m/s, fig. 5.12 shows the concentration of product gases in the outlet with flow time. The Maximum value of hydrogen concentration reached in outlet is 0.66mol/m^3 . Figure 5-13 shows the concentration of glycerol in outlet with flow time. Glycerol concentration decreases with flow time and reaching the concentration of 0.7mol/m^3 at 4 second. Figure 5-14 shows the conversion of glycerol with flow time. Glycerol conversion increases with flow time and reaching a value of 0.38 at 4 second.

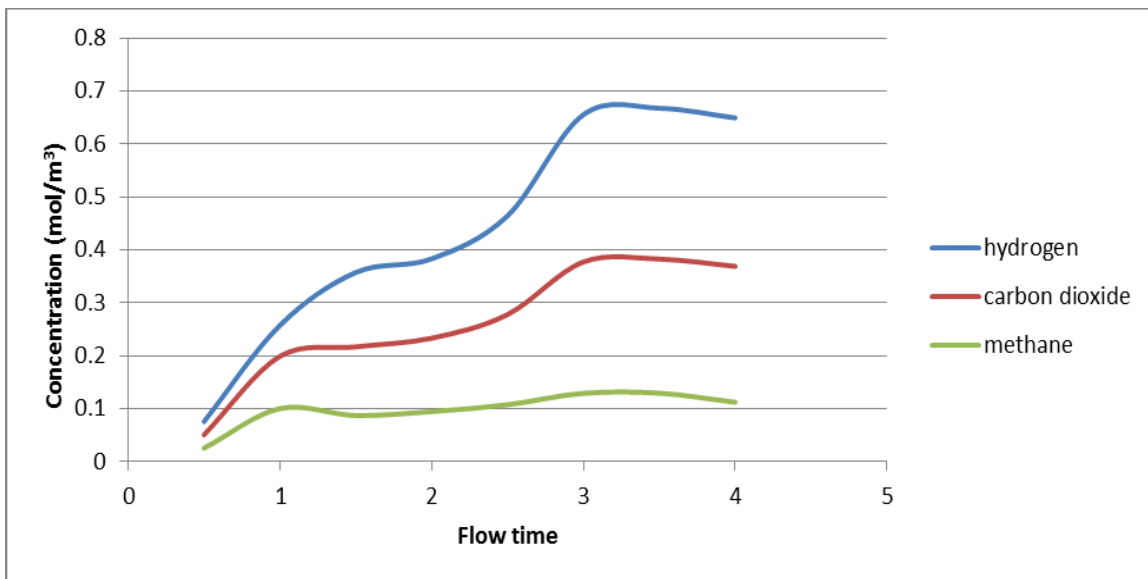


Figure 5.12: Product gases concentration with flow time ($v=0.6\text{m/s}$, $s/c=2:1$, $T=600^{\circ}\text{C}$).

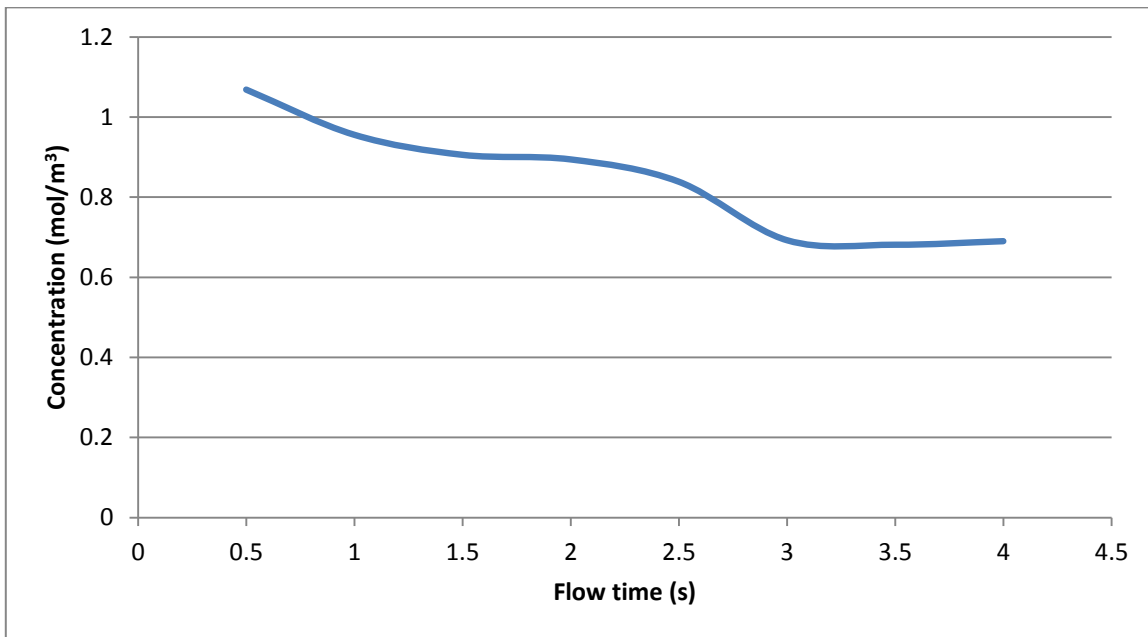


Figure 5.13: Glycerol concentration in outlet with flow time ($v=0.6\text{m/s}$, $s/c=2:1$, $T=600^{\circ}\text{C}$).

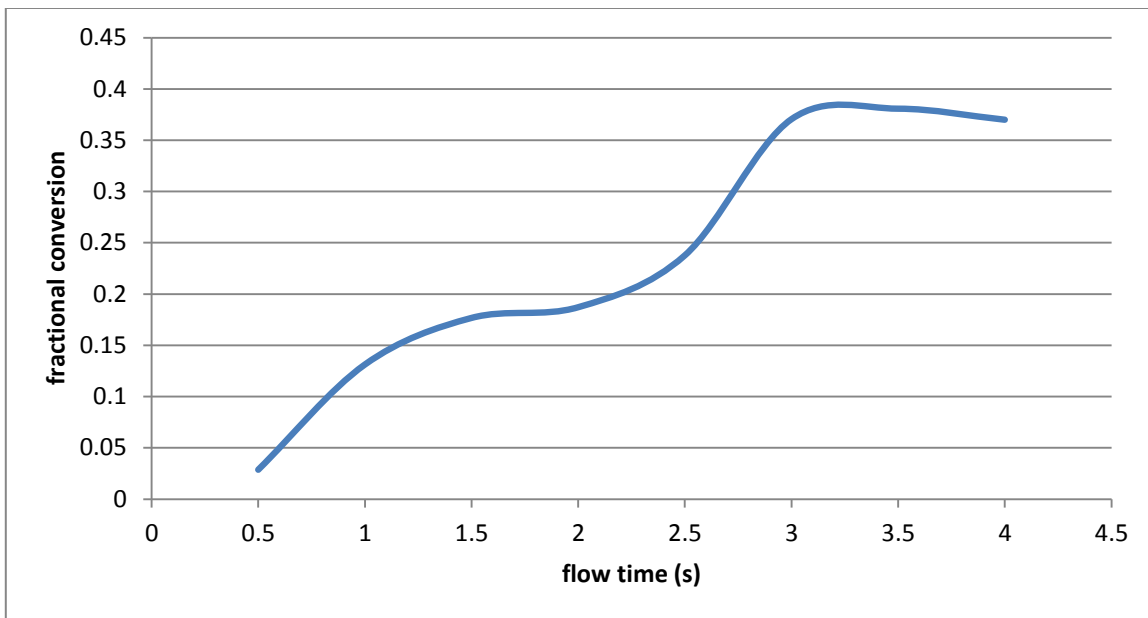


Figure 5.14: Glycerol conversion with flow time ($v=0.6\text{m/s}$, $s/c=2:1$, $T=600^{\circ}\text{C}$).

Figure 5-15 shows the effect of variation in inlet mixture feed velocity on maximum hydrogen concentration in the outlet. It can be seen that as velocity increases from 0.5m/s to 0.6 m/s the

maximum hydrogen concentration obtained in outlet from 0.81mol/m³ to 0.66mol/m³. Figure 5-16 shows the effect of changing inlet velocity of feed mixture on glycerol conversion. The glycerol conversion decreases from 47% to 38% on changing the velocity from 0.5m/s to 0.6 m/s. This decrease in hydrogen concentration in outlet and glycerol conversion obtained can be attributed to the decrease in the residence time for reactants in the reactor thus giving less time for reaction to occur.

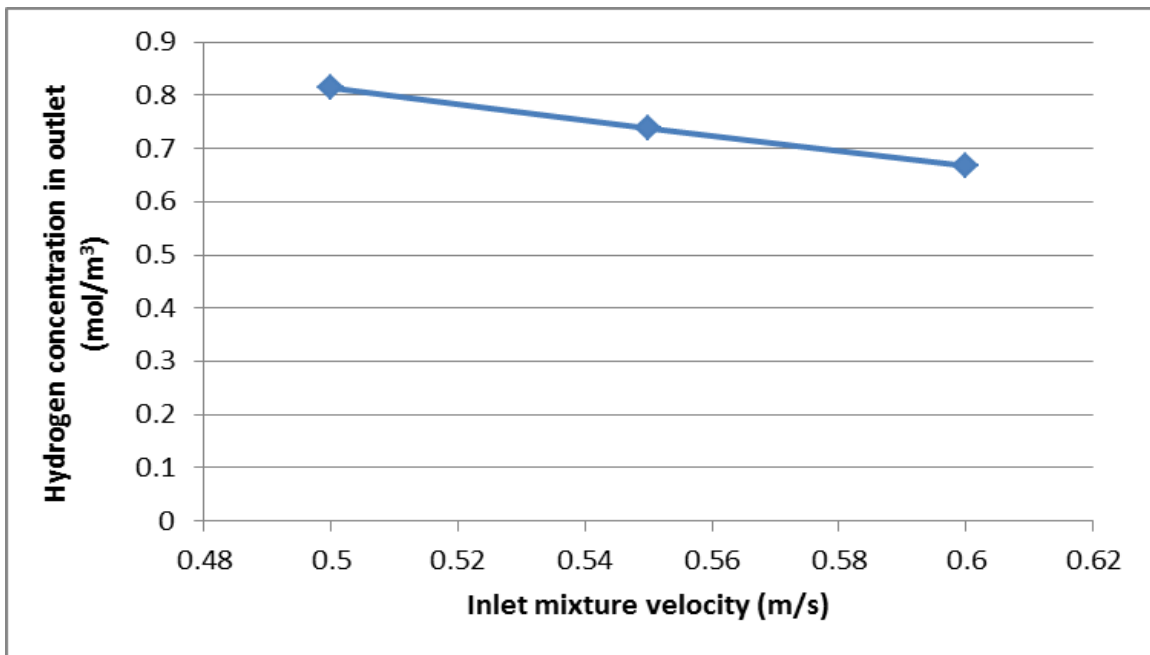


Figure 5.15: Hydrogen concentration in outlet variation with inlet mixture velocity.

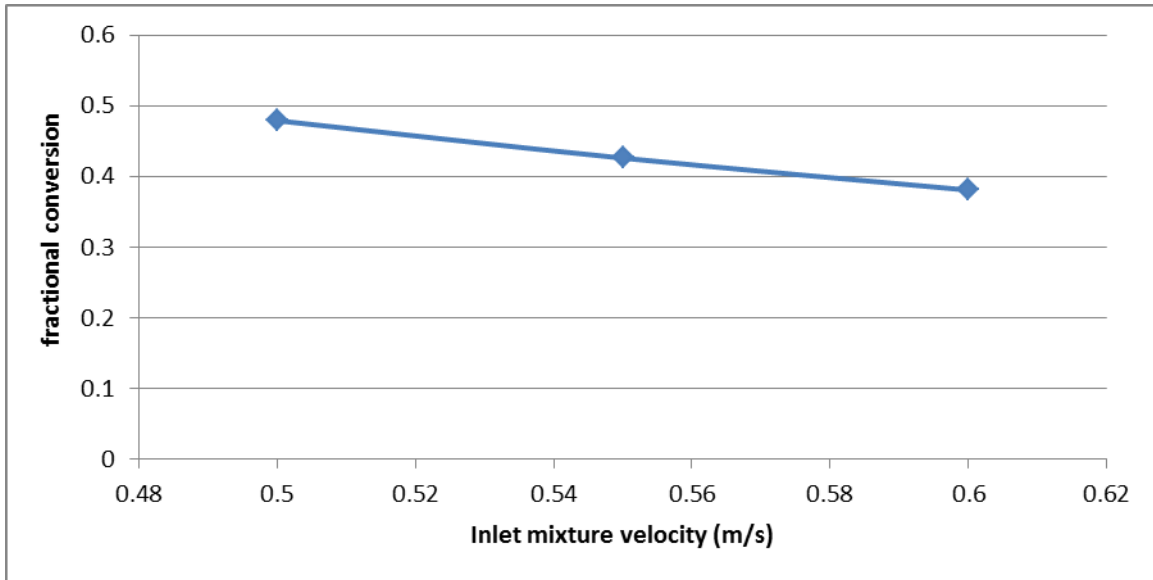


Figure 5.16: Glycerol conversion variation with inlet velocity.

5.3.2 Variation of steam to carbon ratio (s/c) in the inlet mixture

The molar ratio of steam to carbon is varied to see its effect on maximum hydrogen concentration in outlet and glycerol conversion obtained. Simulations are carried out at three values of steam to carbon ratio 2:1, 3:1 and 4:1 at inlet mixture velocity of 0.5 m/s and at temperature of 600⁰C.

For steam to carbon ratio of 2:1 the product concentration and glycerol conversion curves are given from figure 5-6 to 5-8.

Figure 5-17 shows the product gas concentration in the outlet with flow time at steam to carbon ratio (s/c) of 3:1. The maximum value of hydrogen reached in the outlet is 0.854mol/m³. Figure 5-18 and 5-19 gives the concentration of glycerol in outlet and glycerol conversion with flow time respectively. The values of glycerol concentration and glycerol conversion are 0.53mol/m³ and 52.5% respectively

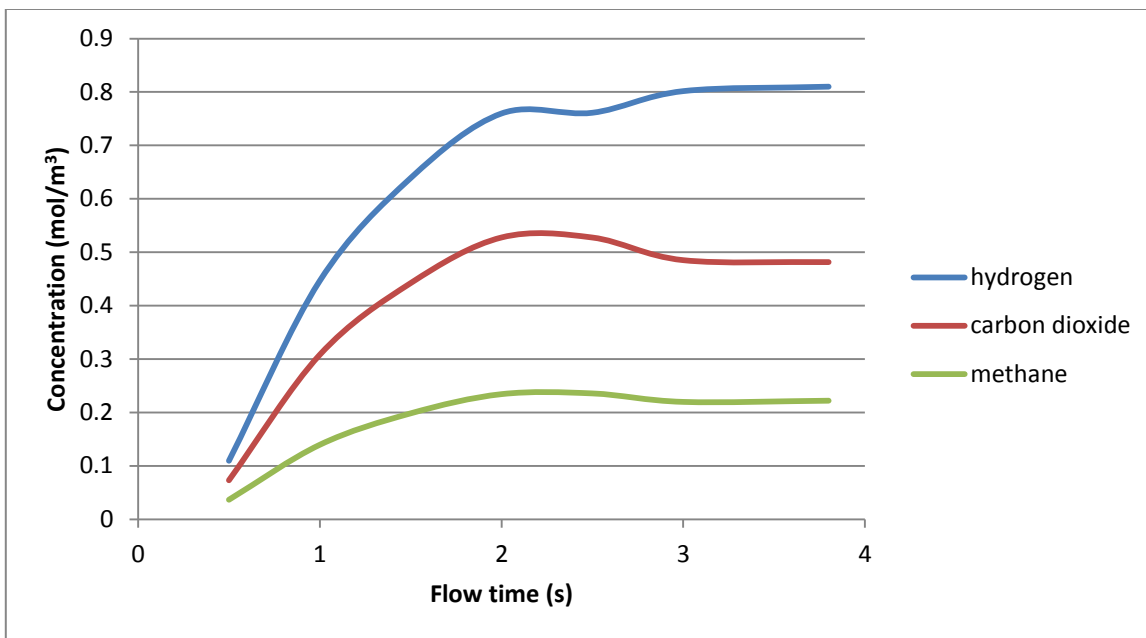


Figure 5.17: Product gases concentration with flow time ($v=0.5\text{m/s}$, $s/c=3:1$, $T=600^{\circ}\text{C}$).

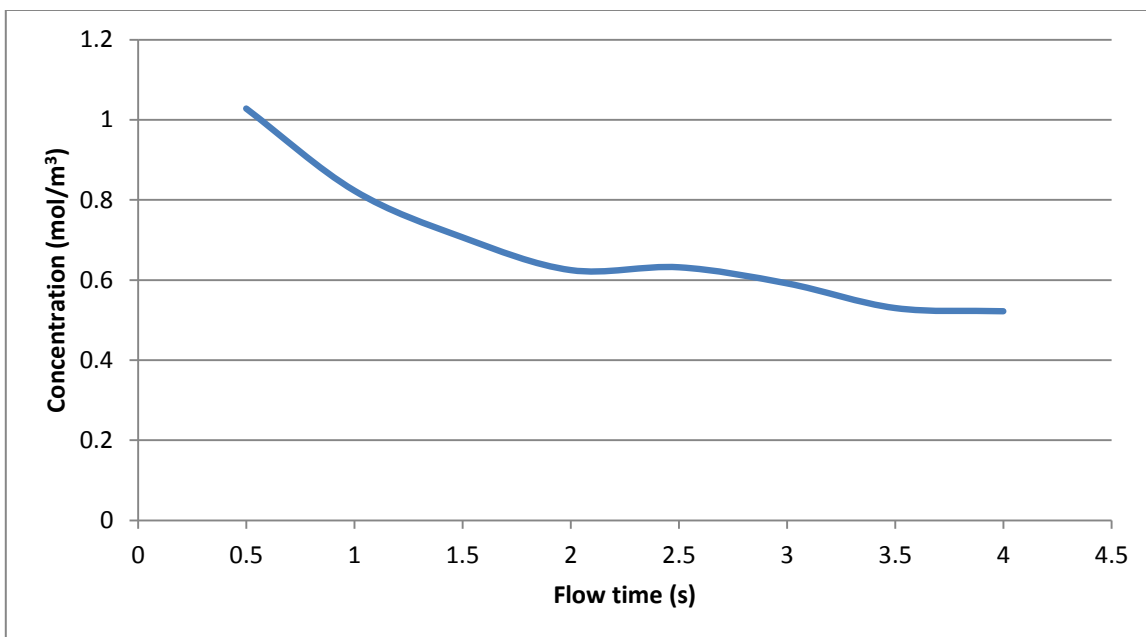


Figure 5.18: Glycerol concentration in outlet with flow time ($v=0.5\text{m/s}$, $s/c=3:1$, $T=600^{\circ}\text{C}$).

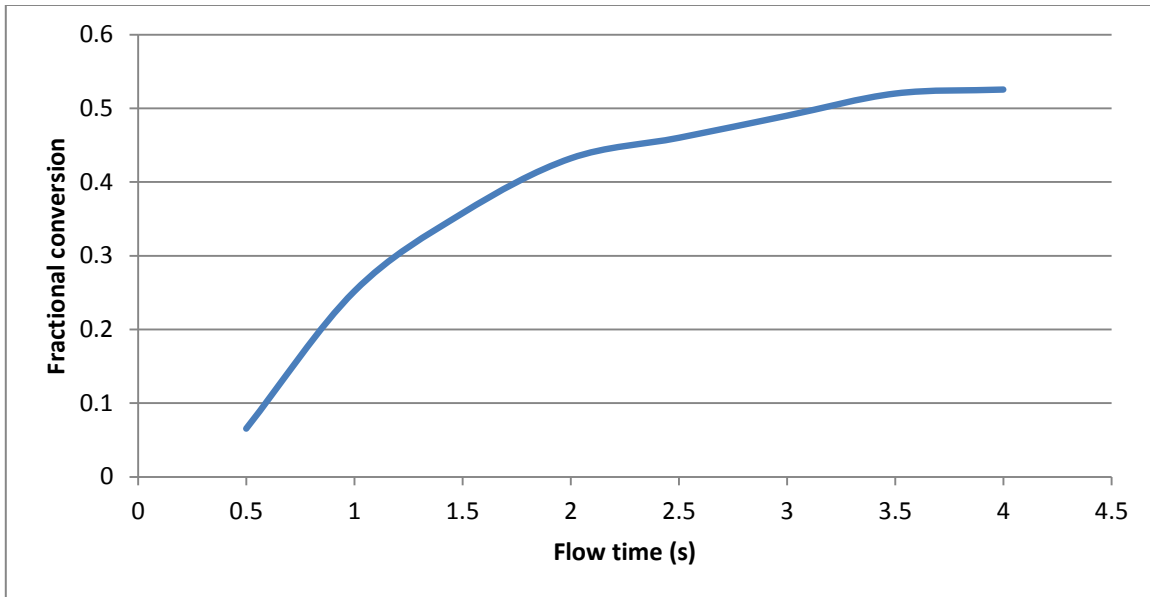


Figure 5.19: Glycerol conversion with flow time ($v=0.5\text{m/s}$, $s/c=3:1$, $T=600^{\circ}\text{C}$)

Figure 5.20 shows the product gas concentration in the outlet with flow time at steam to carbon ratio (s/c) of 4:1. The maximum value of hydrogen reached in the outlet is 1.07mol/m^3 . Figure 5.21 and 5.22 gives the concentration of glycerol in outlet and glycerol conversion with flow time respectively. The values of glycerol concentration and glycerol conversion are 0.43mol/m^3 and 62.0 % respectively

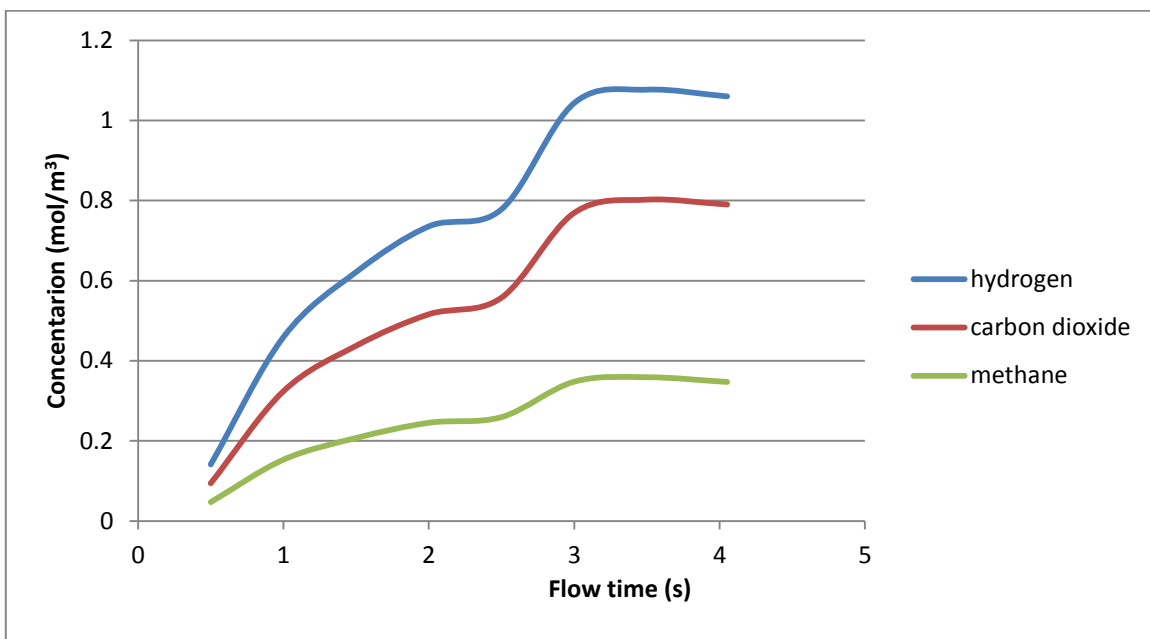


Figure 5.20: Product gases concentration with flow time ($v=0.5\text{m/s}$, $s/c=4:1$, $T=600^{\circ}\text{C}$).

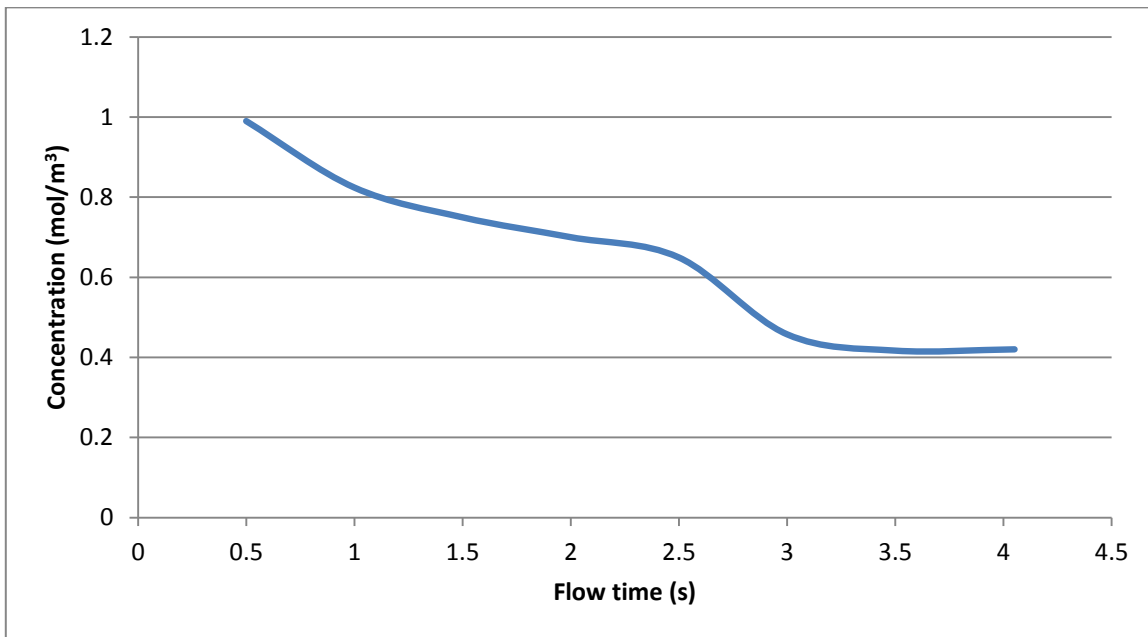


Figure 5.21: Glycerol concentration in outlet with flow time ($v=0.5\text{m/s}$, $s/c=4:1$, $T=600^{\circ}\text{C}$).

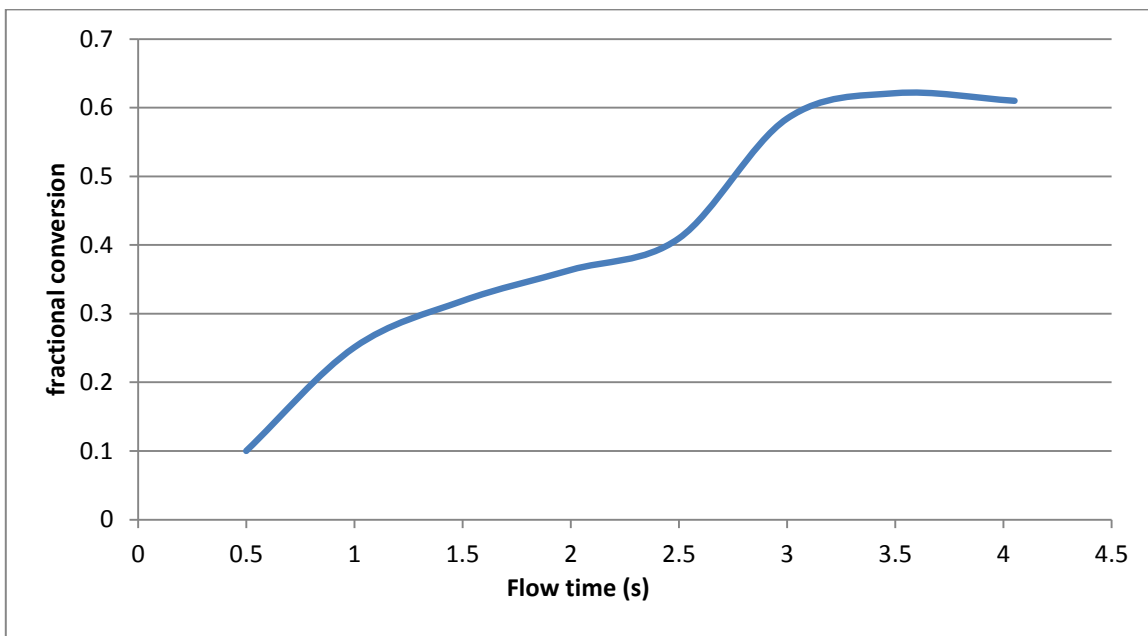


Figure 5.22: Glycerol conversion in outlet with flow time ($v=0.5\text{m/s}$, $s/c=4:1$, $T=600^{\circ}\text{C}$)

Figure 5.23 shows the effect of changing steam to carbon ratio from 2:1 to 4:1 on maximum hydrogen concentration obtained in the outlet. It can be seen that on changing steam to carbon ratio from 2:1 to 4:1 maximum hydrogen concentration in outlet increases from 0.81mol/m^3 to 1.07mol/m^3 .

Figure 5-24 shows the effect of changing steam to carbon ratio from 2:1 to 4:1 on glycerol conversion obtained. It can be seen that on changing steam to carbon ratio from 2:1 to 4:1 glycerol conversion increases from 47% to 62%.

The increase in glycerol conversion and hydrogen production with increasing steam to carbon ratio can be attributed to enhanced water gas shift reaction occurring in presence of excess steam feeding.

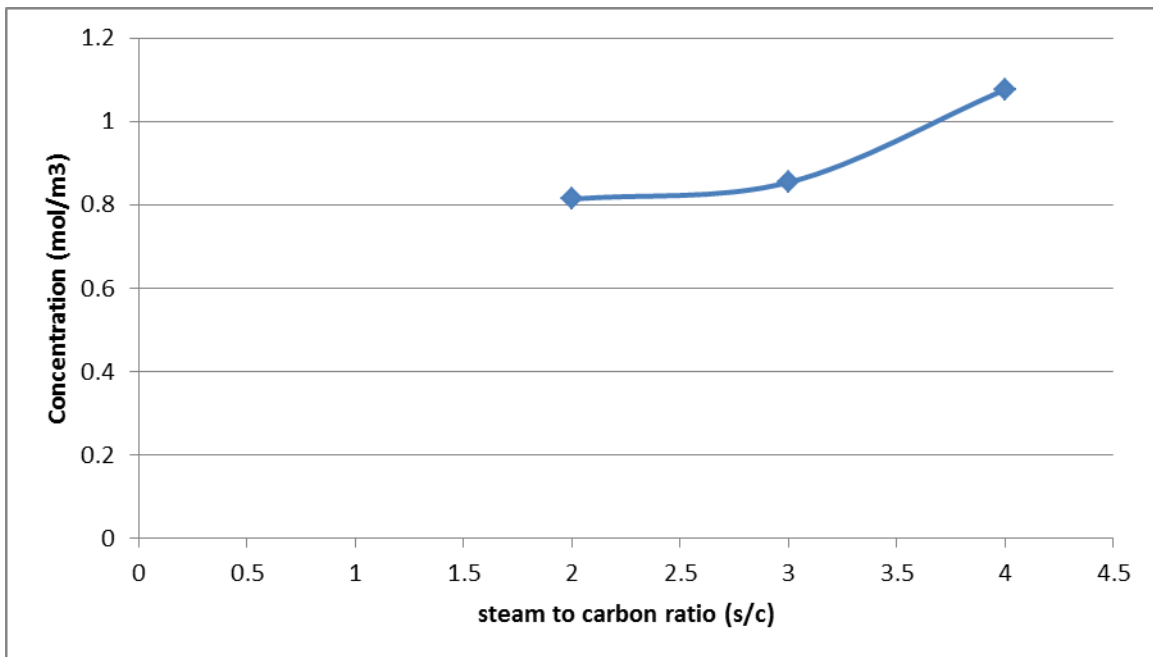


Figure 5.23: Variation of hydrogen concentration in outlet with s/c ratio.

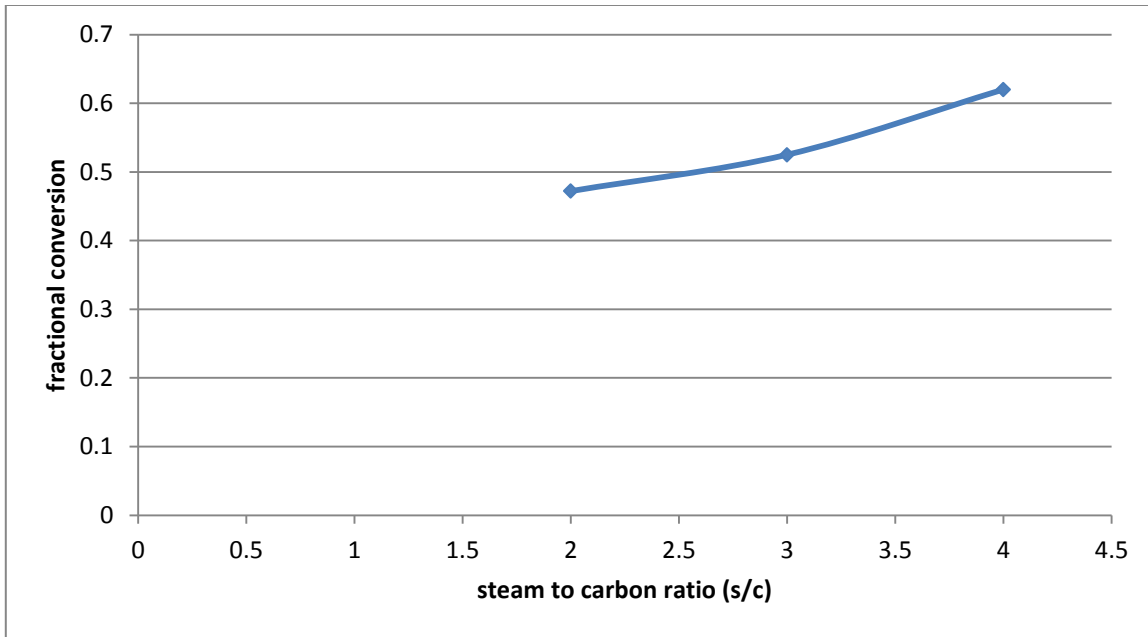


Figure 5.24: Variation of Glycerol conversion with s/c ratio

5.3.3 Variation of reaction temperature

The reactor temperature variation can affect the maximum product gases concentration in outlet and glycerol conversion obtained. The simulations has been carried out at three values of temperature (600°C , 650°C and 700°C) to investigate the effect of temperature on hydrogen formation and glycerol conversion at inlet mixture velocity of 0.5 m/s and steam to carbon ratio (s/c) of 2:1.

The figures showing variation of product concentration and glycerol conversion with flow time for temperature 600°C are from figure 5-6 to figure 5-8.

Figure 5-25 shows the concentration of product gases in outlet with flow time at 650°C . The concentration of products increases with flow time and hydrogen concentration reaching a maximum value of $0.89\text{mol}/\text{m}^3$. Figure 5-26 shows glycerol conversion with flow time at temperature 650°C . It can be seen that maximum glycerol conversion reached is 51%.

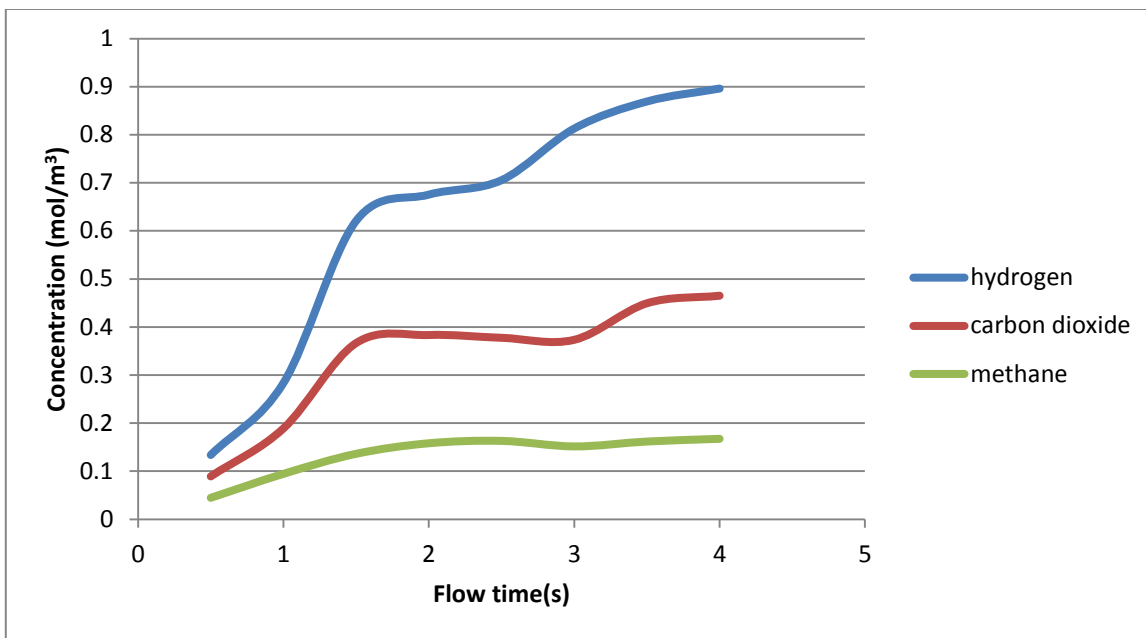


Figure 5.25: Product gases concentration with flow time ($v=0.5\text{m/s}$, $s/c=2:1$, $T=650^{\circ}\text{C}$)

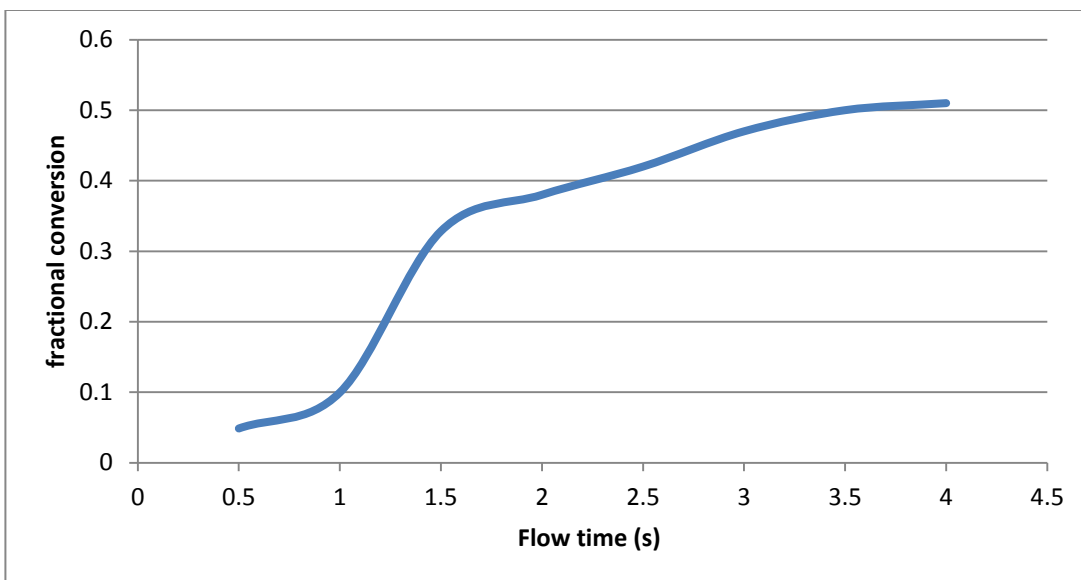


Figure 5.26: Glycerol conversion with flow time ($v=0.5\text{m/s}$, $s/c=2:1$, $T=650^{\circ}\text{C}$)

Figure 5-27 shows the concentration of product gases in outlet with flow time at 700⁰C. The concentration of products increases with flow and hydrogen concentration reaching a maximum value of 1.02 mol/m³. Figure 5-28 shows glycerol conversion with flow time at temperature 700⁰C. It can be seen that maximum glycerol conversion reached is 55%.

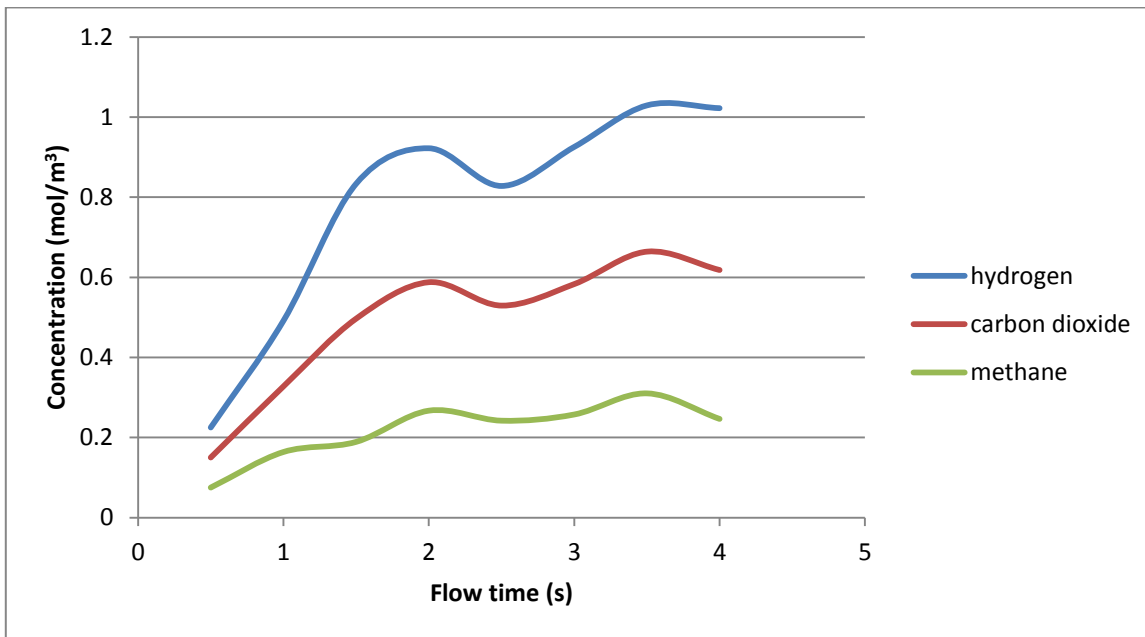


Figure 5.27: Product gases concentration with flow time ($v=0.5\text{m/s}$, $s/c=2:1$, $T=700^{\circ}\text{C}$)

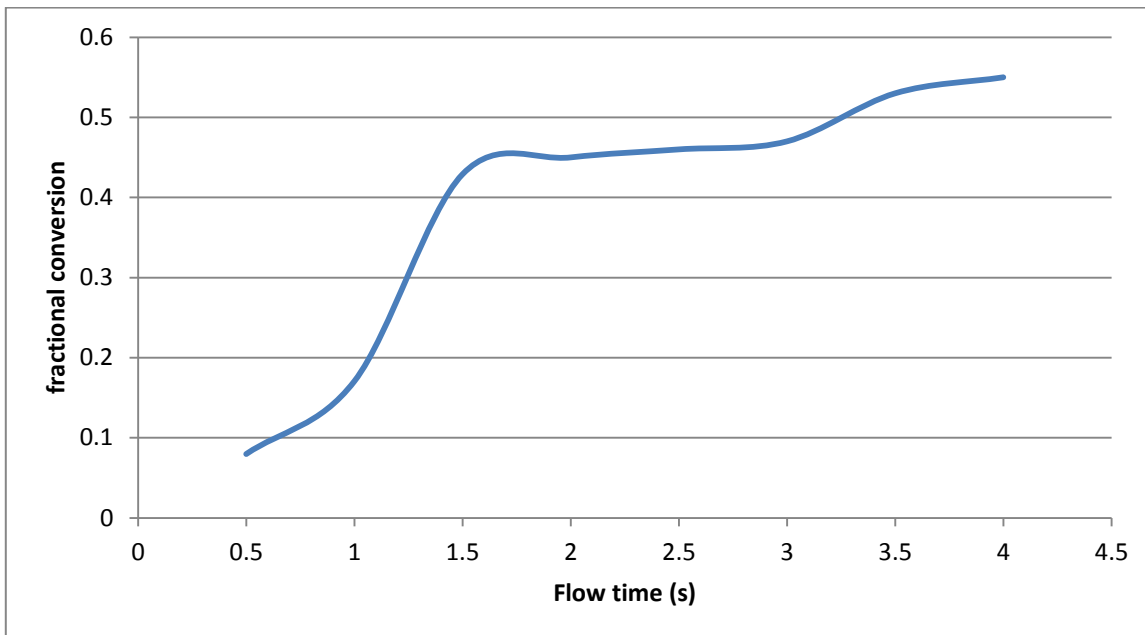


Figure 5.28: Glycerol conversion with flow time ($v=0.5\text{m/s}$, $s/c=2:1$, $T=700^{\circ}\text{C}$)

Figure 5-28 shows the change in maximum hydrogen concentration obtained in the outlet with temperature change from 600⁰C to 700⁰C. It can be seen that maximum hydrogen concentration in outlet increases from 0.81mol/m³ to 1.02mol/m³ on increasing reactor temperature from 600⁰C to 700⁰C. Figure 5-29 shows the increase in glycerol conversion from 47% to 55% on increasing the temperature from 600⁰C to 700⁰C. The reason for this change in hydrogen formation and glycerol conversion with temperature can be the increase the reaction rates constant with increase in temperature.

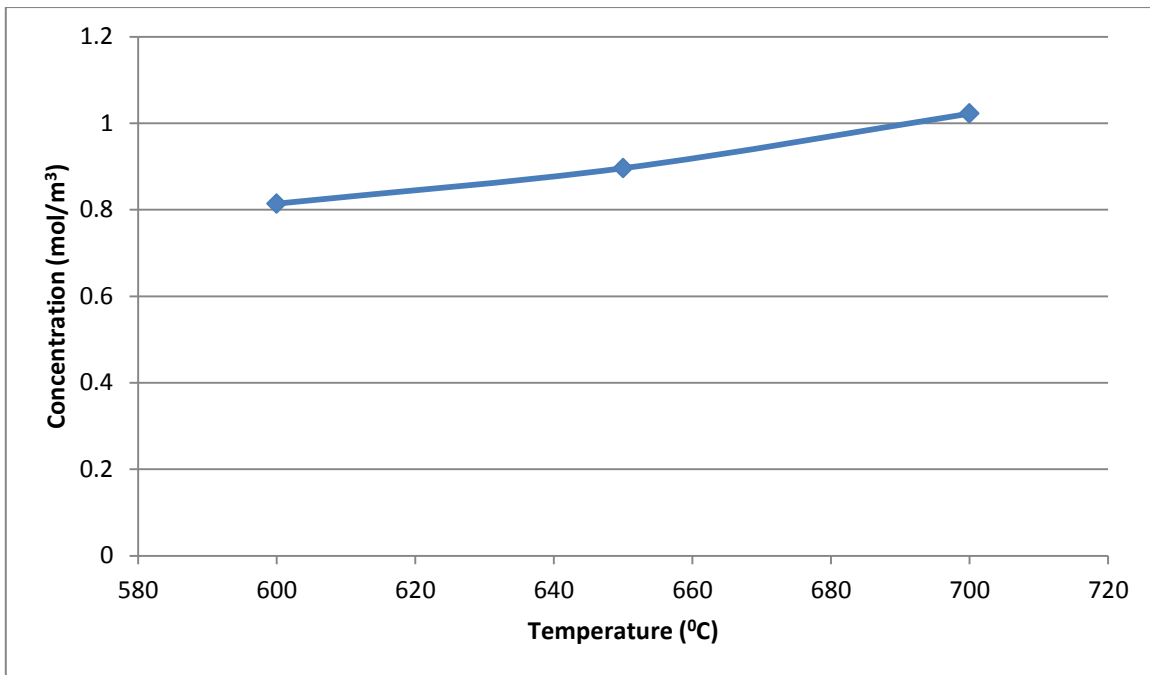


Figure 5.29: Variation of hydrogen concentration in outlet with temperature.

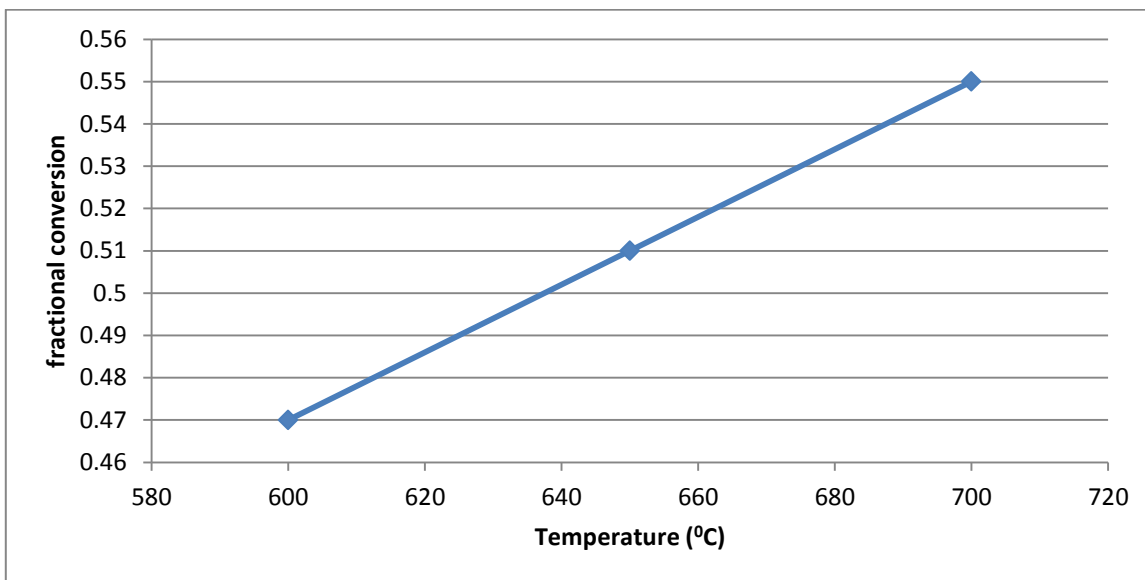


Figure 5.30: Variation of glycerol conversion with temperature

6 Conclusion and Recommendations

6.1 Conclusion

Glycerol is a by-product of few industrial processes like biodiesel production, saponification of fats and others. Biodiesel has become very famous recently due to its environmental benefits thus leading to large amount of crude glycerol as by-product. This has become very cheap and might also become a waste problem. Glycerol to hydrogen conversion is seen as an attractive route to use this waste glycerol and also hydrogen is a clean energy source. Glycerol steam reforming is the most attractive conversion processes.

In this work glycerol steam reforming in a fluidized bed reactor is modeled and simulated in commercial available CFD solver FLUENT 13.0(ANSYS). The Eulerian-Eulerian model with an additional equation for kinetic term is used to model the reactor. Chemical reactions are modeled by laminar finite rate model. The product gases consist of H₂, CO₂, CH₄ and CO in small amounts. The results of simulation show that

- The glycerol conversion and hydrogen formation predicted by simulation were in good agreement with the experimental data.
- Hydrodynamics showed the formation of clusters of solid phase thus making reactor heterogeneous in nature.
- Variation in inlet mixture feed velocity showed that with the increase in inlet velocity, glycerol conversion and hydrogen formation decreases.
- Variation in steam to carbon molar feed ratio showed that with the increase in s/c ratio, glycerol conversion and hydrogen formation increases.
- Variation in reactor temperature showed that with increase in temperature, glycerol conversion and hydrogen formation increases.

The modeling and simulation of glycerol steam reforming reaction in a fluidized bed reactor using CFD technique can be a useful tool in determining the behavior of the reactor and help in operating and maintaining a bench-scale reactor.

6.2 Recommendations

The following recommendations can be made on basis of above study:

- The behavior of the reactor can more accurately be predicted by investigating more into the interaction between the solid and gas phase in fluidized bed reactor.
- Different catalyst can be used in the simulation thus determining the catalytic effect on glycerol conversion and hydrogen formation.
- Atmospheric circulating fluidized bed reactor can be used instead of bubbling fluidized bed reactor.

7 References

- [1] Fangrui Ma, Milford A. Hannab “Biodiesel production: a review” Department of Food Science and Technology, University of Nebraska, Lincoln, NE, USA, 1999.
- [2] Hao Wang, Xiaodong Wang, Maoshuai Li, Shuirong Li, Shengping Wang, “Thermodynamic analysis of hydrogen production from glycerol autothermal reforming” School of Chemical Engineering and Technology, Tianjin University, 2009.
- [3] Sushil Adhikari, Sandun Fernandoa, Steven R. Gwaltneyb, S.D. Filip Toa, R. Mark Brickac et al. “Athermodynamic analysis of hydrogen production by steam reforming of glycerol” Department of Agricultural and Biological Engineering, Mississippi State University, 2007
- [4] Baocai Zhang, Xiaolan Tang, Yong Li, Yide Xu, Wenjie Shen “Hydrogen production from steam reforming of ethanol and glycerol over ceria supported metal catalysts” State Key Laboratory of Catalysis, Dalian Institute of Chemical Physics, China, 2006.
- [5] Francisco Pompeo, Gerardo Santori, Nora N. Nichio “Hydrogen and/or syngas from steam reforming of glycerol. Study of platinum catalysts” Universidad Nacional de La Plata, Argentina, 2010.
- [6] V. Chiodo, S. Freni, A. Galvagnob, N. Mondelloa, F. Frusteri “Catalytic features of Rh and Ni supported catalysts in the steam reforming of glycerol to produce hydrogen” DIIM, Università degli Studi di Catania, Italy, 2010.
- [7] Binlin Dou, Valerie Dupont, Paul T. Williams, Haisheng Chen, Yulong Ding “Thermogravimetric kinetics of crude glycerol” School of Process, Environmental and Materials Engineering, University of Leeds, LS2 9JT, UK, 2008.
- [8] Kaihu Hou, Ronald Hughes “The kinetics of methane steam reforming over a Ni/ α -Al₂O catalyst” Chemical Engineering Unit, University of Salford, Maxwell Building, The Crescent, Salford, Manchester M5 4WT, UK, 2000.
- [9] Binlin Dou, Valerie Dupont, Gavin Rickett, Neil Blakeman, Paul T. Williams, et al. “Hydrogen production by sorption-enhanced steam reforming of glycerol” School of Process,

Environmental and Materials Engineering, University of Leeds, Woodhouse Lane, Leeds LS2 9JT, UK, 2008.

[10] Binlin Dou, Gavin L. Rickett, Valerie Dupont, Paul T. Williams, Haisheng Chen, et al. "Steam reforming of crude glycerol with in situ CO₂ sorption" School of Process, Environmental and Materials Engineering, University of Leeds, Leeds LS2 9JT, UK, 2009.

[11] Binlin Dou, Valerie Dupont, and Paul T. Williams "Computational Fluid Dynamics Simulation of Gas Solid Flow during Steam Reforming of Glycerol in a Fluidized Bed Reactor" Energy and Resources Research Institute, University of Leeds, Leeds, LS2 9JT, U.K, 2008.

[12] Sushil Adhikari, Sandun Fernando, Agus Haryanto "Production of hydrogen by steam reforming of glycerin over alumina-supported metal catalysts" Department of Agricultural and Biological Engineering, Mississippi State University, Mississippi State, USA, 2007.

[13] Sushil Adhikari, Sandun D. Fernando, Agus Haryanto "Kinetics and Reactor Modeling of Hydrogen Production from Glycerol via Steam Reforming Process over Ni/CeO₂ Catalysts" Department of Biosystems Engineering, Auburn University, Auburn, USA, 2008.

[14] Parag N. Sutar, Prakash D. Vaidya, Alirio E. Rodrigues "Glycerol-Reforming Kinetics Using a Pt/C Catalyst" Department of Chemical Engineering, Institute of Chemical Technology, Mumbai, India, 2010.

[15] Ravi Sundari, Prakash D. Vaidya "Reaction kinetics of glycerol steam reforming using a Ru/Al₂O₃ catalyst" Department of Chemical Engineering, Institute of Chemical Technology, Nathalal Parekh Road, Matunga, Mumbai, India, 2012.

[16] Sebastian Zimmermann, Fariborz Taghipour "CFD Modeling of the Hydrodynamics and Reaction Kinetics of FCC Fluidized-Bed Reactors" Department of Chemical & Biological Engineering, University of British Columbia, 2360 East Mall, Vancouver, B.C., V6T 1Z3 Canada, 2005.

[17] Haisheng Chen, Tianfu Zhang, Bilin Dou, Valerie Dupont, Paul Williams, et al. "Thermodynamic analyses of adsorption-enhanced steam reforming of glycerol for hydrogen production" School of Process, Environmental and Materials Engineering, University of Leeds, Leeds LS2 9JT, UK, 2009.

- [18] Sushil Adhikari, Sandun D. Fernando, S. D. Filip To, R. Mark Bricka, Philip H. Steele, " Conversion of Glycerol to Hydrogen via a Steam Reforming Process over Nickel Catalysts " Department of Agricultural and Biological Engineering, Mississippi State University, 2007.
- [19] Li Y, Wang W, Chen B, Cao Y. " Thermodynamic analysis of hydrogen production via glycerol steam reforming with CO₂ adsorption." Int J Hydrogen Energy 2010.
- [20] Chaouki J, Gonzalez A, Guy C, Klvana D. "Two-phase model for a catalytic turbulent fluidized-bed reactor: application to ethylene synthesis." Chem Eng Sci 1999.
- [21] Zou LM, Guo YC, Chan CK. "Cluster-based drag coefficient model for simulating gasesolid flow in a fast-fluidized bed." Chem Eng Sci 2008.
- [22] Lettieri P, Felice RD, Pacciani R, Owoyemi O. "CFD modeling of liquid fluidized beds in slugging mode." Powder Technol 2006.
- [23] Benyahia S, Arastoopour H, Knowlton TM, Massah H. Simulation of particles and gas flow behavior in the riser section of a circulating fluidized bed using the kinetic theory approach for the particulate phase. Powder Technol 2000.
- [24] Cornelissen JT, Taghipour F, Escudie R, Ellis N, Grace JR. CFD modeling of a liquid solid fluidized bed. Chem Eng Sci 2007.
- [25] Fluent, Inc.. FLUENT 6.3 user's guide. Lebanon, NH: Fluent, Inc.; 2006.